Atmos. Chem. Phys. Discuss., https://doi.org/10.5194/acp-2018-1339
Manuscript under review for journal Atmos. Chem. Phys.
Discussion started: 25 January 2019

Atmospheric Chemistry and Physics
Open Access
Discussions

Evaluation and comparison of MAIAC, DT and DB aerosol products over China

Ning Liu[1], Bin Zou[1,2], Huihui Feng[1,2], Yuqi Tang[1], Yu Liang[1]

[1]School of Geosciences and Info-Physics, Central South University, Changsha, 410083, China
[2]Key Laboratory of Metallogenic Prediction of Nonferrous Metals and Geological Environment Monitoring（Central South University), Ministry of Education, Changsha, 410083, China

Correspondence to: Bin Zou (210010@csu.edu.cn); Huihui Feng (hhfeng@csu.edu.cn);

Abstract. A new Multiangle Implementation of Atmospheric Correction (MAIAC) algorithm has been applied in Moderate Resolution Imaging Spectroradiometer (MODIS) sensor and recently provides globally high spatial resolution Aerosol Optical Depth (AOD) products at 1 km. Meanwhile, several improvements are modified in classical Dark Target (DT) and Deep Blue (DB) aerosol retrieval algorithms in MODIS collection 6.1 products. However, validation and comparison for MAIAC, DT and DB algorithms is still lacking in China. In this paper, a comprehensive assessment and comparison of AOD products at 550 nm wavelength based three aerosol retrieval algorithms in MODIS sensor using ground-truth measurements from Aerosol Robotic Network (AERONET) sites over China during 2000 to 2017 is presented. In general, after quality assurance (QA) filter, the coefficient of determination (R^2=0.854), correlation coefficient (R=0.929), root-mean-square error (RMSE=0.178), mean bias (Bias=0.019) and the fraction fall within expected error (Within_EE=67.10%, EE=±(0.05+0.15×AOD)) results for MAIAC algorithm show better accuracy than those from DT and DB algorithms. While the R2, R, RMSE, Bias and Within_EE of DT algorithm are 0.817, 0.930, 0.192, 0.077, 55.36%, respectively, those corresponding statistics for DB algorithm are 0.827, 0.921, 0.190, 0.018, 63.32%. Moreover, the spatiotemporal completeness for MAIAC (29.69%) product is also better than DT (8.00%) and DB (19.50%) products after QA filter. In addition, the land type dependence characteristic, view geometry dependence, spatiotemporal retrieval accuracy and spatial variation pattern difference for three products are also analyzed in details.

1 Introduction

Aerosols are multi-compartment system consisting of suspended solid and liquid particles in the atmosphere which plays an important role in radiative forcing (Rajeev et al., 2001), regional climate (Qian et al., 1999) and urban air pollution (Dominici et al., 2014). Aerosol optical depth (AOD) is the key aerosol optical parameter which defines as vertical integration of aerosol extinction coefficient from ground to top of atmosphere (TOA). Ground measurements from Aerosol Robotic Network (AERONET) provide high quality multiband aerosol optical and microphysical properties at 15 min sampling frequency from global scale (Holben et al., 2001). High quality ground measurements are often employed to validate satellite aerosol products (Chu et al., 2002) and provide regional aerosol model for satellite aerosol retrieval algorithm (Levy et al., 2013). However, it cannot grasp high aerosol spatial variability due to its sparse ground stations where spatial variability information is still necessary. Satellite monitoring can remedy this drawback with spatial continuous measurements.

Moderate Resolution Imaging Spectroradiometer (MODIS) sensor with its multiband detection ability from visible band to thermal infrared spectrum band (Salomonson et al., 1989) can detect aerosol properties well. With Terra satellite and Aqua satellite carrying MODIS sensor successfully launch in 2000 and 2002 respectively, it has stored over 17 year globally historical monitored data. Recently, a new Multiangle Implementation of Atmospheric Correction (MAIAC) algorithm has applied in MODIS sensor which provides high spatial resolution aerosol data at 1 km (Lyapustin et al., 2018). In the meantime, some important improvements in classical Dark Target (DT, Mattoo et al., 2017) and Deep Blue (DB, Hsu, 2017) aerosol retrieval algorithms are revised in MODIS collection 6.1 products. However, any satellite aerosol retrieval algorithms are all under some hypothesis and approximation, the accuracy should be validated before applying one satellite aerosol product in its related studies.

China is undergoing severe aerosol pollution and numerous studies in aerosol pollution uses MODIS collection 6.0 aerosol retrievals to mapping aerosol pollution and analyze its spatiotemporal trend (Fang et al., 2016; Ma et al., 2014; He et al., 2018; Zou et al., 2016, 2019; Zhai et al., 2018). A little researches have applied 1km MAIAC aerosol retrievals to map finer aerosol concentration in regional China, e.g. Yangtze River Delta (Xiao et al., 2017) and Shandong province (Li et al., 2018). Before widely applying MAIAC and C6.1 products in China, the accuracy difference, applicable condition of three aerosol retrievals should be recognized firstly to guide users to utilize these products. Recently, the global validation (Lyapustin et al., 2018) and regional validation in south America (Martins et al., 2017) and north America (Superczynski et al., 2017) for MAIAC product show more than 66% of retrievals fall within in the expected error (EE=±(0.05+0.05×AOD)) limits which means good accuracy for MAIAC products. However, there is not any evaluation for DT, DB algorithm in collection 6.1 and detailed evaluation or comparison for three products in China is still scarce due to they have only released recently.

In this context, we devote oneself to provide a first comprehensive understanding aerosol retrieval uncertainties for MAIAC, DT and DB products in China from spatiotemporal accuracy differentiation pattern, spatiotemporal completeness, land type dependence characteristic, view geometry dependence characteristic aspect, etc. The following paper is organized as follows: section 2 briefly introduces three satellite products with theirs retrieval algorithm and ground AERONET data, validation approach is clarified in section 3, and section 4 provides a detailed validation results and discussion. The conclusion are presented in section 5.

2 Data Description

Three aerosol products, e.g. MAIAC, DT and DB are stored in Hierarchical Data Format (*.hdf) file, and we obtain corresponding *.hdf file in China region during 2000 to 2017 from NASA Earthdata Search website (https://search.earthdata.nasa.gov/search/). Ground measurement aerosol data obtained from AERONET website (https://aeronet.gsfc.nasa.gov/) are used to validate the accuracy of three satellite aerosol products. Besides, land cover data from Geographical Information Monitoring Cloud Platform (GIMCP, http://www.dsac.cn/) are utilized to analyze land cover dependency for three satellite aerosol products.

2.1 DT products

DT algorithm retrieves AOD parameter based on the assumption that the surface reflectance in two visible bands, e.g. 470 nm and 644 nm, presents good linear relationship with surface reflectance in shortwave infrared (SWIR) band, e.g. 212 nm, in dark dense vegetated area, and the measurement in SWIR band is transparent with aerosol particle (Kaufman et al., 1997, Levy et al., 2013). Then the surface and aerosol information can be decoupled from TOA spectral reflectance. Compared with DT algorithm in collection 6.0, DT algorithm in collection 6.1 mainly revised the surface characterization over land surface when the urban percentage is larger than 20% (Gupta et al., 2016).

DT algorithm produces two resolution aerosol products in collection 6.0 and 6.1, e.g. 3 km×3 km and 10 km×10 km. The two resolution products share the same retrieval protocol except using different retrieval box. For example, 10 km product organizes 20×20 group pixels with three aforementioned band measurements at 500 resolution into retrieval box, on the contrary, 3 km product combines three band measurement in 6×6 pixel group into retrieval box (Remer et al., 2013). The comparison between 10 km product and 3 km product from collection 6.0 in global scale (Remer et al., 2013) and China region (He et al., 2017) show that the accuracy of 10 km product is superior to one of 3 km product in spite of 3 km product provide finer resolution aerosol retrievals. In this study, we take 10 km product of the newest collection 6.1 version from Terra satellite into consideration and scientific data set (SDS) named “Image_Optical_Depth_Land_And_Ocean” without quality assurance (QA) filter and “Optical_Depth_Land_And_Ocean” with QA filter (QA>1 for ocean and QA>3 for land) are extracted to compare the accuracy with QA filter and without QA filter.

2.2 DB products

DB algorithm retrieves AOD parameter under the hypothesis that the surface reflectance at deep blue band, e.g. 412 nm, is much smaller than longer bands over bright surface such as urban and desert region (Hsu et al., 2004). Firstly, DB algorithm retrieves 1 km aerosol properties using global surface reflectance database at visible bands, e.g. 412 nm, 470 nm and 650 nm, and then aggregates 1 km pixels into 10 km scale. In collection 6.0, the surface reflectance database is improved using the knowledge of normalized difference vegetation index, scattering angle and season (Hsu et al., 2013). The ability of retrieving aerosol data over bright surface for DB algorithm greatly expand the coverage of aerosol retrieval. The general principles for collection 6.1 DB product are still same with those in collection 6.0 version. The major improvements for collection 6.1 DB product are in radiometric calibration, heavy smoke detection, artifact reduction over heterogeneous terrain, surface model in elevated terrain and regional/seasonal aerosol optical models (Hsu, 2017).

Here, SDS named "Deep_Blue_Aerosol_Optical_Depth_550_Land" without QA filter and "Deep_Blue_Aerosol_Optical_Depth_550_Land_Best_Estimate" with QA filter (QA=2, 3 for land) in collection 6.1 from Terra satellite are selected for our study. Solar zenith angle in "Solar_Zenith" SDS datasets, view zenith angle in "Sensor_Zenith" SDS datasets, solar azimuth angle in "Solar_Azimuth" SDS datasets, sensor azimuth angle in "Sensor_Azimuth" SDS datasets and scattering angle in "Scattering_Angle" SDS datasets are also picked up to analysis view geometry dependence for DT and DB products.

2.3 MAIAC products

MAIAC algorithm relies on the assumption that surface reflectance changes slowly over time and shows highly variability over space, whereas aerosol loading changes very fast in time and varies only on a limited space scale. The main procedure of MAIAC is as follow: firstly, MAIAC resamples MODIS L1B measurement into a fixed 1 km grid, then it adopts 4~16 day time series of resampled MODIS measurement to retrieve surface Ross–Thick Li–Sparse (RTLS) bidirectional reflectance distribution function (Lucht et al., 2000) using measurement in SWIR band. After that, the linear spectral regression coefficient (SRC) between 470 nm and 212 nm for each 1 km grid are retrieved instead of using empirical regression coefficient in DT algorithm. Finally, the AOD parameter in 470 nm can be retrieved by searching the minimum of a spectral residual between theoretical TOA reflectance of look-up table and measurement in red and SWIR bands. The AOD is originally retrieved in 470 nm and the AOD parameter in 550 nm is computed using AOD parameter in 470 nm based on spectral properties, which is expressed by regional aerosol model from MAIAC look-up table. The detailed MAIAC algorithm can be found in Lyapustin et al., 2011.

Data used in this study is from "Optical_Depth_055" and "AOD_QA" SDS datasets and data from Terra satellite is collected. The datatype of "AOD_QA" SDS datasets is a 16-bit unsigned integer and the best retrieved quality can be selected if 8~11 byte of "AOD_QA" SDS datasets bits "0000" (Lyapustin et al., 2018). Solar zenith angle in "cosSZA" SDS datasets, view zenith angle in "cosVZA" SDS datasets, relative azimuth angle in "RelAZ" SDS datasets and scattering angle in "Scattering_Angle" SDS datasets are also picked up to analysis view geometry dependence for MAIAC products.

2.4 AERONET data

AERONET is a global ground-based aerosol monitoring network which provide continuous aerosol optical and microphysical properties at 15 min sampling rate with high accuracy of ~-0.01 to 0.021 (Eck et al., 1999). But it does not record aerosol measurement at 550 nm, we interpolate AOD parameter at 550 nm using Ångström exponent in the two neighboring bands at 500 nm and 675 nm. AERONET provide three quality level data, e.g. level 1.0, level 1.5 and level 2.0, in version 3. Here, we only choose quality-assured level 2.0 data as ground-truth data to validate satellite data. Figure 1 shows the locations of the selected 50 AERONET sites across China in this study. Table 1 reports site name, longitude, latitude of the selected sites.

Atmos. Chem. Phys. Discuss., https://doi.org/10.5194/acp-2018-1339
Manuscript under review for journal Atmos. Chem. Phys.
Discussion started: 25 January 2019

Atmospheric Chemistry and Physics
Discussions

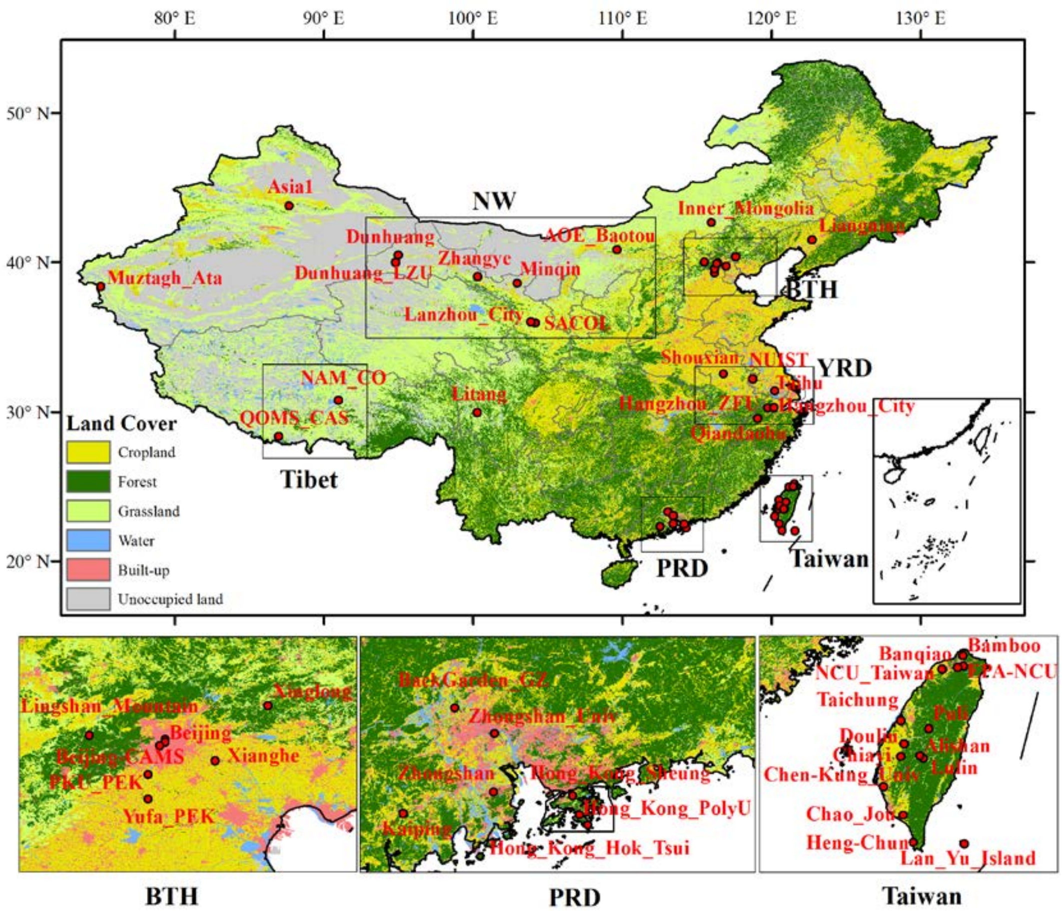

Figure 1: The locations of selected AERONET sites around China displayed in the land cover map in 2013. BTH: Beijing-Tianjin-Heibei; YRD: Yangtze River Delta; PRD: Pearl River Delta; NW: northwestern China.

Site	Long.	Lat.	Period	Site	Long.	Lat.	Period
NCU_Taiwan	121.19	24.97	1998-2013	Qiandaohu	119.05	29.56	2007-2009
Taipei_CWB	121.54	25.01	2000-2018	Hangzhou_City	120.16	30.29	2008-2009
Beijing	116.38	39.98	2001-2018	Kaiping	112.54	22.32	2008-2008
Dunhuang	94.79	40.04	2001-2001	Shouxian	116.78	32.56	2008-2008
Inner_Mongolia	115.95	42.68	2001-2001	Zhangye	100.28	39.08	2008-2008
Lan_Yu_Island	121.56	22.04	2001-2001	Lanzhou_City	103.85	36.05	2009-2010
XiangHe	116.96	39.75	2001-2018	QOMS_CAS	86.95	28.37	2009-2018
Chen-Kung_Univ	120.20	22.99	2002-2018	Zhongshan	113.38	22.52	2009-2009
EPA-NCU	121.19	24.97	2004-2018	Beijing_RADI	116.38	40.00	2010-2018
Chao_Jou	120.53	22.51	2005-2005	Minqin	102.96	38.61	2010-2010

Hong_Kong_PolyU	114.18	22.30	2005-2018	Litang	100.26	29.98	2011-2011
Liangning	122.70	41.51	2005-2005	Muztagh_Ata	75.04	38.41	2011-2011
Taichung	120.49	24.11	2005-2005	Zhongshan_Univ	113.39	23.06	2011-2012
Taihu	120.22	31.42	2005-2018	Beijing-CAMS	116.32	39.93	2012-2018
BackGarden_GZ	113.02	23.30	2006-2006	Dunhuang_LZU	94.96	40.49	2012-2012
Lulin	120.87	23.47	2006-2018	Hong_Kong_Sheung	114.12	22.48	2012-2018
NAM_CO	90.96	90.96	2006-2018	AOE_Baotou	109.63	40.85	2013-2018
PKU_PEK	116.18	39.59	2006-2008	Chiayi	120.50	23.50	2013-2018
SACOL	104.14	35.95	2006-2013	Heng-Chun	120.70	22.05	2013-2015
Xinglong	117.58	40.40	2006-2014	Puli	120.97	23.97	2013-2013
Yufa_PEK	116.18	39.31	2006-2006	Lingshan_Mountain	115.50	40.05	2014-2015
Asia1	87.65	43.78	2007-2007	Douliu	120.54	23.71	2015-2018
Hangzhou-ZFU	119.73	30.26	2007-2009	Alishan	120.81	23.51	2016-2016
Hong_Kong_Hok_Tsui	114.26	22.21	2007-2010	Bamboo	121.54	25.19	2016-2017
NUIST	118.72	32.21	2007-2010	Banqiao	121.44	25.00	2017-2017

Table 1: The selected AERONET sites used in this study. Long. and Lat. is abbreviate for Longitude and Latitude.

2.5 Land cover data

One key difficulties in aerosol retrieval algorithm is to decouple surface and atmosphere information in satellite apparent reflectance. Land cover information greatly affects atmosphere properties (Xu et al., 2018; Feng et al., 2019). Understanding the uncertainties for a satellite aerosol retrieval algorithm in different land cover type is necessary. GIMCP land cover data with 30 m resolution in the year of 2000, 2005, 2008, 2010, 2013 are used in this study. The first level of GIMCP land cover data includes cropland, forest, grassland, water, built-up and unoccupied land. Among them, unoccupied land includes desert, gobi, saline-alkali soil, swampland, bare land and bare rock gravel which is mainly includes bright surface. The high spatial resolution and abundant land cover type support our studies. Figure 1 shows the first level land cover type across China mainland in 2013.

3. Evaluation method

3.1 The selected spatiotemporal window

There is only a little matchup data between satellite data and ground data if using direct matching method, e.g. use only one pixel where AERONET station located and ground measurement at the exact satellite overpassed time, due to large missing data in AERONET or satellite data and time delay between satellite overpass time and AERONET sampling time. Therefore, with the assumption that aerosol information is homogeneous in a limited spatial lag and temporal lag, a suitable spatiotemporal window is often adopted to increase the matchup data number. That is to say, satellite measurements in the spatial window around AERONET station are averaged and ground measurements in the temporal window centered the satellite overpass time are averaged.

For 10 km DT and DB product, the selected spatial window is often 50 km×50 km and temporal window is ±30 min (Ichoku et al., 2002, He et al., 2017, Tao et al., 2015). For MAIAC product, Matins et al., testified five different spatial window, e.g. 3 km, 15 km, 25 km, 75 km and 125 km, and four temporal window, e.g. 30 min, 60 min, 90 min and 120 min in validating MAIAC product over south America (Matins et al., 2017). The result shows 25 km×25 km and ±60 min are reasonable for Terra satellite. For comparison with 10 km DT and DB products, we select 30 km×30 km as spatial window which is close to the best spatial window for MAIAC product and employ the best temporal window ±30 min of 10 km product because we also notice that the validation accuracy is very close for ±30 min and ±60 min temporal window in Matins et al.'s result although the matchup data number of ±60 min temporal window is more than one of ±30 min temporal window (Matins et al., 2017).

3.2 Land cover type for AERONET sites

The first level of GIMCP land cover data are used to label AERONET site group. Due to the selected 30 km×30 km spatial window in section 3.1, we follow Matins et al.'s work and label AERONET sites if the proportion of one land cover type exceed 50% in the spatial window around AERONET site. If there is no dominant land cover type, we define the land cover type for this AERONET site as mixed group (Matins et al., 2017). Except for the defined first level type in GIMCP land cover data, we found there are some coastal AERONET sites which the dominant region is ocean, so we define the land cover type for these sites as ocean group.

Table 2 shows land cover type for each AERONET site in 2013. There is no land cover type change for most sites except for Hangzhou_City, Muztagh_Ata and NAM_CO site. For Hangzhou_City site, the land cover type changes from cropland to mixed group during 2005 to 2008 may due to the process of urbanization. For Muztagh_Ata site, the land cover type changes from unoccupied land to grass land during 2008 to 2010, and the land cover type for NAM_CO site varies from grassland to mixed group between 2008 and 2010. We label each matchup data for the three sites using the land cover type in the nearest year to the AERONET sampling time.

Land Cover	Site	Land Cover	Site	Land Cover	Site
Cropland	Shouxian	Grassland	SACOL	Mixed	NCU_Taiwan
	XiangHe		Asia1		Chen-Kung_Univ
	Liangning		Lanzhou_City		EPA-NCU
	PKU_PEK		QOMS_CAS		Chao_Jou
	Yufa_PEK		Litang		Taichung
	NUIST		Muztagh_Ata		Taihu

Forest	Taipei_CWB		AOE_Baotou	BackGarden_GZ
	Lulin	Built-up	Beijing	NAM_CO
	Xinglong		Beijing_RADI	Hangzhou_City
	Hangzhou-ZFU		Beijing-CAMS	Kaiping
	Qiandaohu	Ocean	Lan_Yu_Island	Zhangye
	Chiayi		Hong_Kong_PolyU	Zhongshan
	Puli		Hong_Kong_Hok_Tsui	Zhongshan_Univ
	Lingshan_Mountain		Heng-Chun	Hong_Kong_Sheung
	Alishan	Unoccupied	Dunhuang	Douliu
	Banqiao	land	Minqin	Bamboo
Grassland	Inner_Mongolia		Dunhuang_LZU	

Table 2: Land cover type for each AEROENT site in 2013.

3.3 Statistical approach

The expected error (EE) envelope are often used to validate the uncertainties the satellite retrievals. If there are more than 66% of retrievals falling within the expected error lines, it means good accuracy. For DT algorithm, the EE envelope is generally defined as ±(0.05+0.15×AOD) over land and over 66% of retrievals meet the defined expected error limits at global scale (Levy et al., 2010, 2013; Remer et al., 2005). In the global scale validation for MAIAC product, there are over 66% of retrievals satisfying the ±(0.05+0.1×AOD) EE limits which show MAIAC accuracy is relatively higher than DT algorithm over land (Lyapustin et al., 2018). In the regional validation of south America for MAIAC product, the EE envelope is defined as ±(0.05+0.05×AOD) and the fraction of retrievals within this EE limits are also over 66% (Matins et al., 2017). In our study, for the purpose of comparing with DT and DB products, we adopt ±(0.05+0.15×AOD) as the EE envelope and calculate the proportion within the EE envelope (Within_EE) using equation (1):

$$\mathrm{AOD} - \mathrm{EE} \leq \mathrm{AOD}_{sat} \leq \mathrm{AOD} + \mathrm{EE}\,, \tag{1}$$

Besides the EE envelope, we also adopt coefficient of determination (R^2) and correlation coefficient (R) to study the correlation between satellite AOD and AERONET AOD. Root mean square error (RMSE) are also utilized to analyze the dispersion degree of the accuracy of satellite AOD. Mean bias (Bias) is used to describe bias of satellite AOD. These statistical indicators are calculated by equation (2)-(5), respectively.

$$R^2 = 1 - \frac{\sum_{i=1}^{N}(\mathrm{AOD}_{sat}-\mathrm{AOD}_{aero})^2}{\sum_{i=1}^{N}(\mathrm{AOD}_{aero}-\overline{\mathrm{AOD}}_{aero})^2}\,, \tag{2}$$

$$R = \frac{\sum_{i=1}^{N}(\mathrm{AOD}_{sat}-\overline{\mathrm{AOD}}_{sat})(\mathrm{AOD}_{aero}-\overline{\mathrm{AOD}}_{aero})}{\sqrt{\sum_{i=1}^{N}(\mathrm{AOD}_{sat}-\overline{\mathrm{AOD}}_{sat})^2\sum_{i=1}^{N}(\mathrm{AOD}_{aero}-\overline{\mathrm{AOD}}_{aero})^2}}\,, \tag{3}$$

$$RMSE = \sqrt{\frac{\sum_{i=1}^{N}(\mathrm{AOD}_{sat} - \mathrm{AOD}_{aero})^2}{N}}, \quad (4)$$

$$Bias = \frac{\sum_{i=1}^{N}(\mathrm{AOD}_{sat} - \mathrm{AOD}_{aero})}{N}, \quad (5)$$

The AOD_{sat} and AOD_{aero} is satellite AOD retrievals and AERONET data respectively. The $\overline{\mathrm{AOD}}_{sat}$ and $\overline{\mathrm{AOD}}_{aero}$ is the corresponding mean value. N is the matchup data number.

4. Result and Discussion

4.1 Overall accuracy comparison

Figure 2 shows the overall evaluation for MAIAC, DT and DB products before QA filter and after QA filter. In total, MAIAC product have more matchup data than ones of DT and DB product which indicates the completeness for MAIAC product maybe higher than ones of DT and DB product. Before QA filter, the statistic show that there are 69.84% of retrievals falling within the EE envelope which means good accuracy for MAIAC products in China. Comparing with DT and DB products, there are only 53.64% and 55.66% of retrievals for DT and DB products. Based on the R statistical result, the result for three products are all larger than 0.9 which means three products are all well correlated with ground-truth AERONET data. Whereas the R^2 statistical result for MAIAC products, e.g. 0.847, shows better than ones for DT and DB products, e.g. lower than 0.8. From the $Bias$ statistical result, there is no significant bias for the overall MAIAC product. However, according to the corresponding bias boxplot in different AOD bins, it seems slightly overestimated when AODs are less than 0.5, slightly underestimated when AODs are between 0.5 and 1. While for DT and DB product, they are seemingly overestimated based on the $Bias$ result. From the corresponding bias boxplot, the mean bias result for each different AOD bins are also almost larger than zero. After QA filter, the correlation for MAIAC product are slightly improved, but the Within_EE result is slightly reduced and RMSE and $Bias$ results become larger. From the corresponding bias boxplot subfigure, the positive mean biases when AODs are less than 0.2 become larger compared with corresponding results before QA filter and the negative biases when AODs are between 0.5 and 1 are reduced. This is the reason for the reduced overall accuracy. The reason for the changes in these statistical indicators will be explained in the section 4.2. For the DT and DB product, the overall accuracies are all improved after QA filter. The improvement for DB product is more obvious than one for DT product. The Within_EE result is improved from 57.66% to 63.32% and the mean biases in the bias boxplot show no obvious overestimated trend after QA filter. However, DT product is still overestimated after QA filter and there is only a little improvement in Within_EE result.

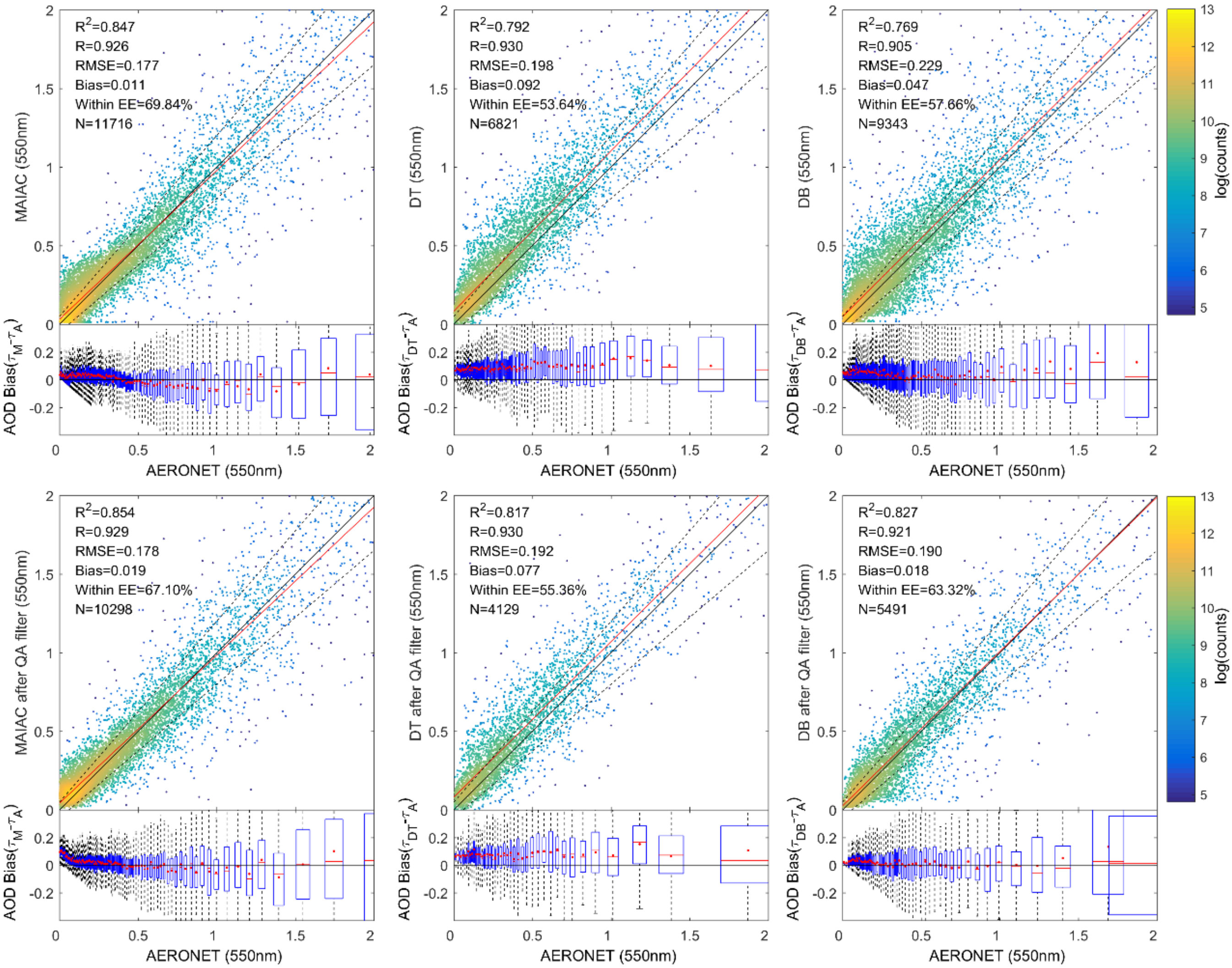

Figure 2: Overall accuracy evaluation of MAIAC, DT and DB AOD versus AERONET AOD at 550nm before and after QA filter. Black line, red line and dashed line in the scatterplot are 1:1 reference line, regression line and expected error (EE=±(0.05+0.15×AOD)) line, respectively. The AOD bias boxplot uses 25% and 75% percentiles with 50 bins. Red points in the boxplot are mean bias for 50 bins.

In order to analyze and comparison the retrieval accuracy in different AOD level for three products, we use Matins et al.'s strategy and four bins with different level are defined: low level (<0.2), moderate level (0.2~0.4), moderate-high level (0.4~0.6) and high level (>0.6) (Matins et al., 2017). Table 3 shows the corresponding statistical result. In low, moderate and moderate-high level, all statistical indicators shows MAIAC product has better accuracy than ones of DT and DB product before QA filter. In the high level, DT product achieve highest correlation with ground-truth data and low RMSE result, but the positive Bias result for DT product show the overestimated phenomenon is more serious than ones of other two products. After QA filer, the accuracy for DB product are higher than other two products in the low level due to the positive bias phenomenon become more severe for MAIAC product in this level. In the moderate level, MAIAC product have the best correlation and lowest RMSE result with a slightly higher positive bias than DB product. In the moderate-high level, MAIAC product still remains the best quality product among the three product. In the high level, the DT product still achieve the best correlation and lowest RMSE with highest positive bias.

AOD level	Data	Before QA filter				After QA filter			
		NOM	Bias	R	RMSE	NOM	Bias	R	RMSE
<0.2	MAIAC	**5541**	**0.032**	**0.580**	**0.086**	**4521**	0.047	0.435	0.084
	DT	2554	0.079	0.469	0.135	1478	0.077	0.455	0.137
	DB	3777	0.057	0.464	0.127	2090	**0.031**	**0.555**	**0.082**
0.2~0.4	MAIAC	**2509**	**0.021**	**0.480**	**0.091**	**2320**	0.016	**0.501**	**0.091**
	DT	1697	0.086	0.386	0.165	1038	0.070	0.361	0.159
	DB	2099	0.039	0.271	0.172	1361	**0.008**	0.408	0.128
0.4~0.6	MAIAC	**1304**	**-0.017**	**0.396**	**0.129**	**1204**	**-0.007**	**0.421**	**0.132**
	DT	989	0.105	0.394	0.202	605	0.081	0.388	0.188
	DB	1249	0.024	0.308	0.218	744	0.012	0.360	0.169
>0.6	MAIAC	**2362**	**-0.033**	0.834	0.346	**2253**	-0.019	0.840	0.336
	DT	1581	0.109	**0.871**	**0.292**	1008	0.081	**0.876**	**0.277**
	DB	2218	0.050	0.825	0.371	1296	**0.010**	0.836	0.330

Table 3: Accuracy evaluation for MAIAC, DT and DB in low level (<0.2), moderate level (0.2~0.4), moderate-high level (0.4~0.6) and high level (>0.6). NOM is the abbreviate for Number Of Match.

4.2 Land cover type dependency analysis

Figure 3 shows scatterplot figure for MAIAC products in different land cover types before and after QA filter. In total, MAIAC retrievals in cropland, built-up, grassland, ocean type are more accurate than forest, unoccupied land and mixed types according to Within_EE results. After QA filter, except for grassland, the accuracy are all improved and the improvement effect in ocean type are more obvious.

The high aerosol loading, e.g. AODs > 1, mostly emerges in the cropland (Figure 3 a-i and a-ii) and built-up (Figure 3 d-i and d-ii) type due to biomass burning in dry season and multiple human activities in built-up area (Zhang et al., 2010). MAIAC retrieves AODs in a very high accuracy in the two land cover types. The R and R^2 result are over 0.93 and 0.84 respectively and the Winthin_EE result show over 74% of retrievals falls into the EE limits. In comparison, retrievals in cropland has a little bias in contrast with a small positive bias in built-up area and RMSE result in built-up area is smaller than ones in cropland area. This high retrieval accuracy in cropland and built-up regions can support relative studies on biomass burning and anthropogenic emissions.

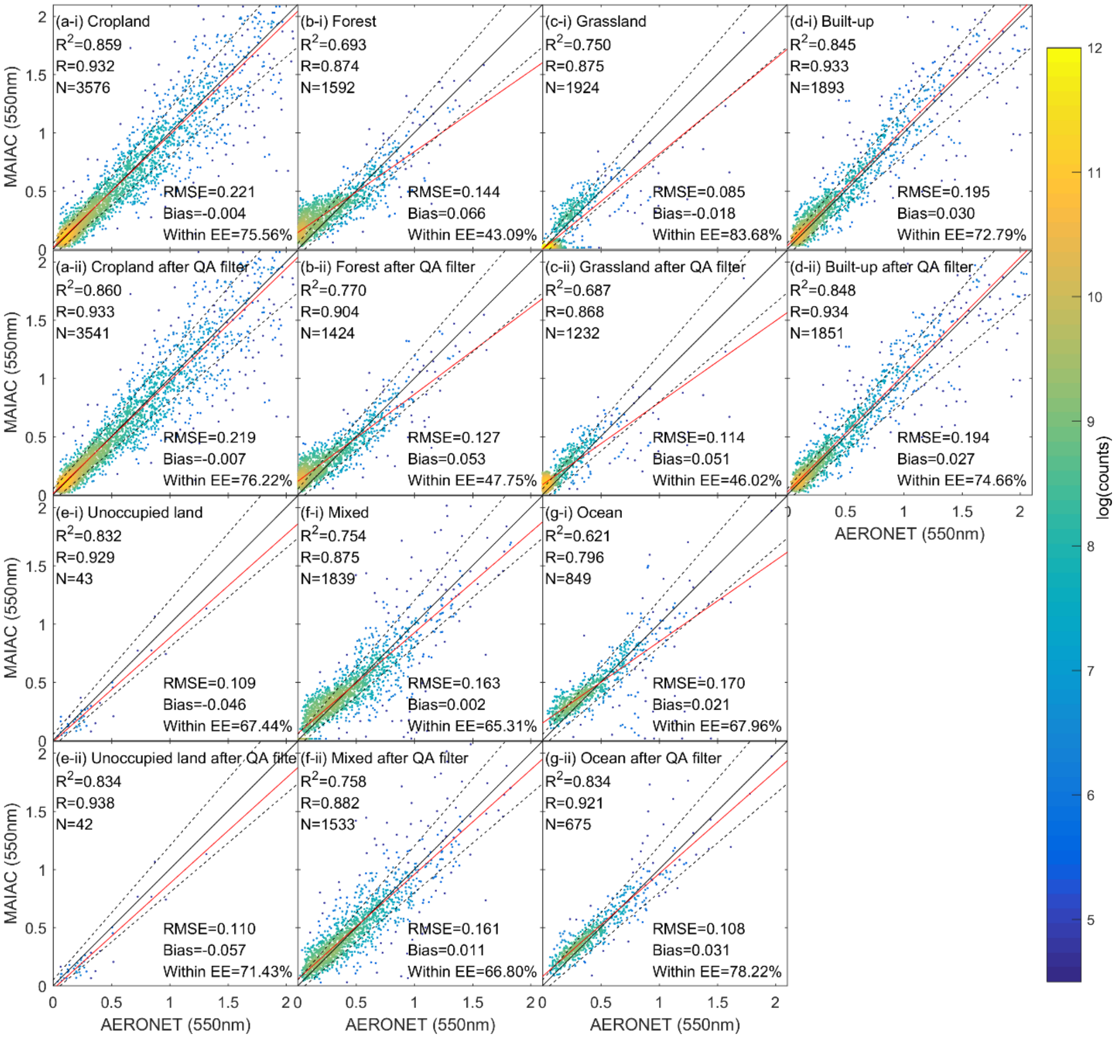

Figure 3. Evaluation MAIAC accuracy at different land cover types before and after QA filter. Black line, red line and dashed line in the scatterplot are 1:1 reference line, regression line and expected error (EE=±(0.05+0.15×AOD)) line, respectively.

In the evergreen forest areas (Figure 3 b-i and b-ii), the retrievals shows good correlation with ground measurements with $R_{no\_QA} = 0.874$, $R_{QA} = 0.904$. However, the R^2 results for without QA filter and QA filter are all lower than 0.8 and there are only around 45% of retrievals falling within the EE envelope. The result is opposite to the conclusion that MAIAC algorithm improves the dark target retrieval accuracy than DT algorithm in Lyapustin et al., 2011 (Lyapustin et al., 2011). In order to eliminate the influence of retrieval accuracy in the specific site, Figure 4 shows scatterplot figure for the forest AERONET site and we ignore the site which the matchup numbers are less than 10. We can see good performance occurs in Chiayi, Qiandaohu and Xinglong sites and the corresponding Within_EE results are all higher than 70%. And the relatively inferior performance sites are Banqiao, Taipei_CWB. After QA filter, the accuracies are improved into 76.19% and 61.79% respectively. The worst performance site is only Lulin site, MAIAC retrievals are systemically higher than ground measurement and there are less than 4% of retrievals falling into EE limits. The percentage of forest type in the Lulin site spatial window are all over 80% in 2000, 2005, 2008, 2010 and 2013. This high proportion of forest type eliminates the influence of other mixed land cover type. The Lulin site is located in Taiwan peninsula, the improper aerosol type in MAIAC algorithm and cloud cover maybe the overestimated reason in Lulin site (Lyapustin et al., 2018).

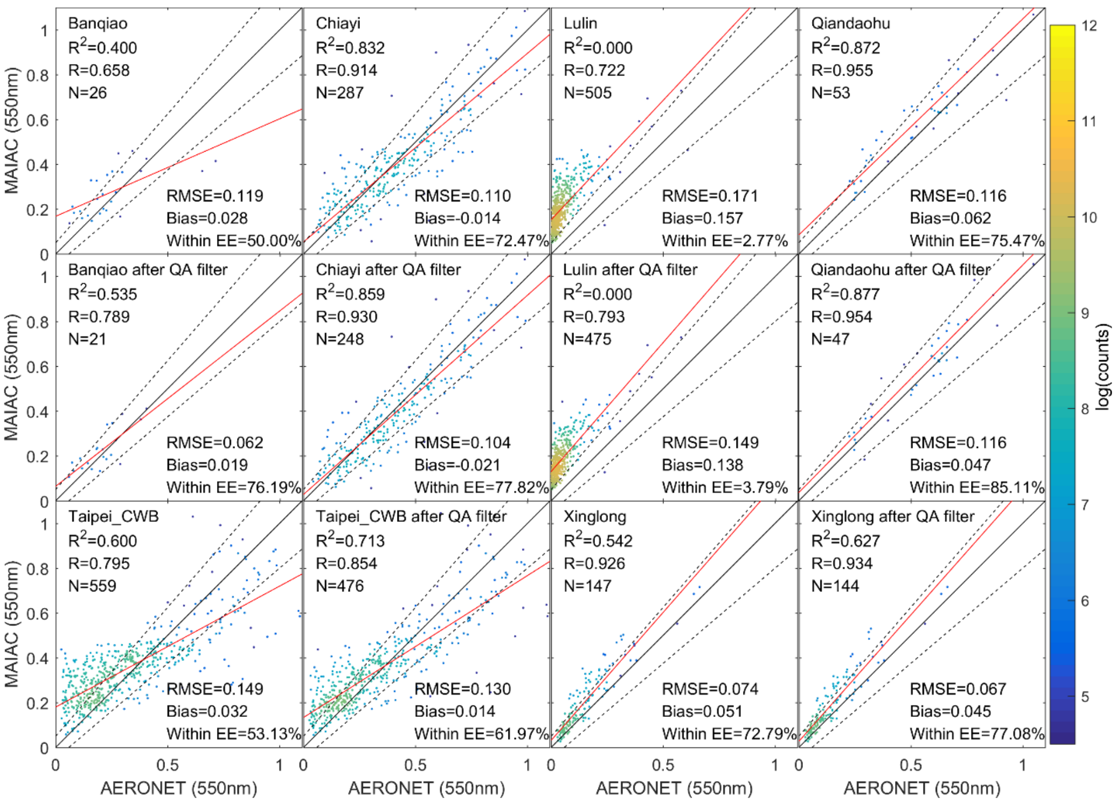

Figure 4. Evaluation of MAIAC accuracy in the forest area for each AERONET site before and after QA filter. Black line, red line and dashed line in the scatterplot are 1:1 reference line, regression line and expected error (EE=±(0.05+0.15×AOD)) line, respectively.

In grassland type (Figure 3 c-i and c-ii), over 83.68% of MAIAC retrievals fall into the EE lines before QA filter, and the R^2=0.750, R=0.875, RMSE=0.085, Bias=-0.018 results are all shows good accuracy in grassland type. But after QA filter, the accuracy was dramatically decreased with Within_EE=46.02%, R^2=0.687, R=0.868, Bias = 0.051 and RMSE=0.114. This is the main reason for some decreased overall statistical results in MAIAC product after QA filter. Note that, there are some underestimated values when AODs are less than 0.5 and these values are discarded after QA filter. But there are emerging some overestimated values when AODs are very small. To find the reason, we also statistic the validation result for each grassland type sites in Figure 5 and ignore the site with less than 10 matchup number. Before QA filter, we found the underestimated values are mainly in NAM_CO and QOMS_CAS sites. The two sites are located in the Tibetan plateau, MAIAC algorithm fill the AOD retrievals using climatology values, e.g. 0.014, in the high altitude regions, e.g. over 4.2 km, and the QA for climatology values is 0111 (Lyapustin et al., 2018). After QA filter, the climatology values are thrown away in NAM_CO site. For QOMS_CAS site, there are still nearly 2.13% of pixels whose altitude is small than 4.2 km in spatial window. MAIAC retrievals in these pixels are overestimated compared with ground measurements. After QA filter, the Within_EE result are decreased from 92.26% to 38.53%. Severe underestimated phenomenon are found in Lanzhou_City site in contrast with positive bias in its closest SACOL site. The small matchup number for Lanzhou_City site may be the reason for underestimated phenomenon. Great improvement is found in Muztagh_Ata site after QA filter.

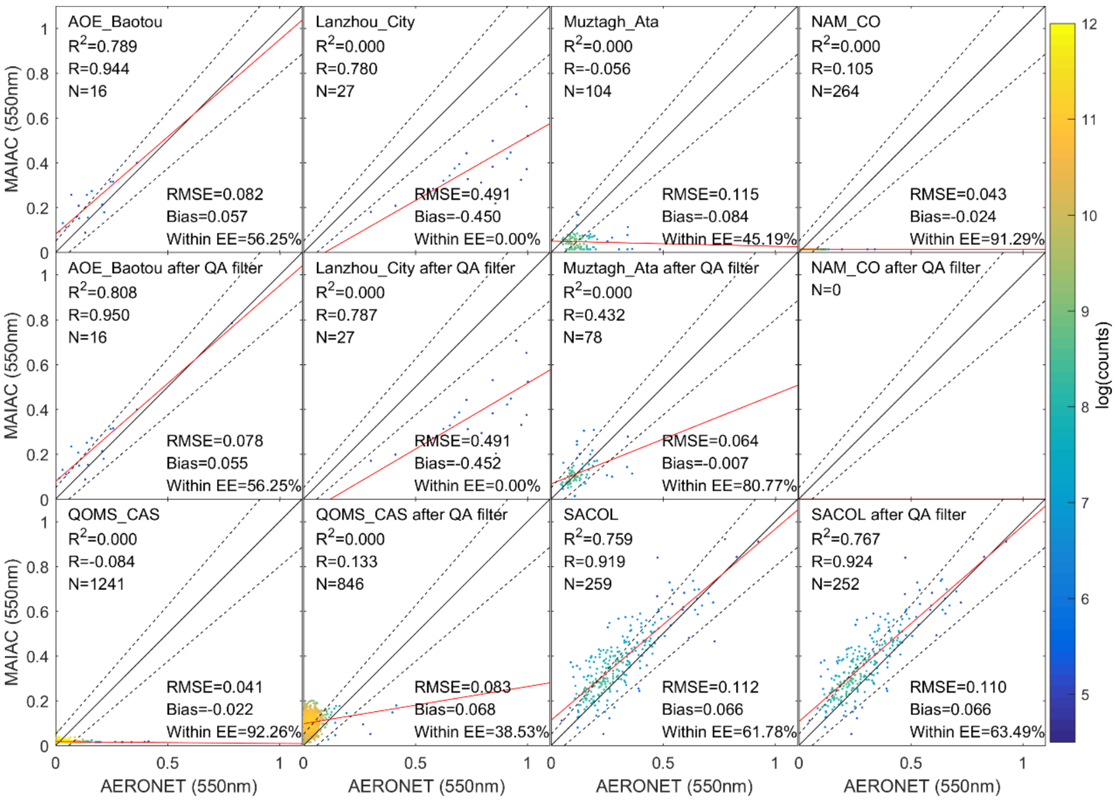

Figure 5. Evaluation of MAIAC accuracy in the grassland area for each AERONET site before and after QA filter. Black line, red line and dashed line in the scatterplot are 1:1 reference line, regression line and expected error (EE=±(0.05+0.15×AOD)) line, respectively.

MAIAC performs good accuracy in the unoccupied land cover type (Figure 3 e-i and e-ii), the Within_EE result is 67.44% and 71.43% before and after QA filter and the R and R^2 results are over 0.9 and 0.8 respectively. Figure 3 f-i and f-ii indicate MAIAC also achieve better performance in the mixed land cover area with Within_EE=66.80% and R=0.882. In the ocean area (Figure 3 f-i and f-ii), MAIAC algorithm retrievals seem overestimated when AODs are small and the R=0.796 result show a little worse than one of other land types. After QA filter, the overestimated values are discarded and the accuracy is greatly improved from R=0.796, Within_EE=67.96% to R=0.921, Within_EE=78.22%.

In comparison with DT and DB products, Table 4 shows validation statistical results of MAIAC, DT and DB products with different land type covers. In cropland area, the accuracy for DT product is evidently better than ones of MAIAC and DB product according to R^2, R, RMSE results. However, it seems overestimated compared with MAIAC product and the

Within_EE result is a little smaller than MAIAC product. In the forest area, DT algorithm also achieve best accuracy compared with MAIAC and DB products. But only 56.23% of retrievals meet the EE limits which is less than DB product. In the grassland type region, the accuracies for three products are all decreased after QA filter and we consider the validations in three products are all influenced by NAM_CO and QOMS_CAS sites. Compared with DT and DB products, MAIAC product obtains the best retrieval accuracy. Owing to the overestimated phenomenon in QOMS_CAS sites after QA filter, the Within_EE result is dramatically dropped from 83.68% to 46.02%. In Built-up, unoccupied land and mixed regions, MAIAC product performs better than DB product and DB product is more accurate than DT product. In ocean region, DT product is obvious accurate than DB and MAIAC products.

			Cropland	Forest	Grassland	Built-up	Unoccupied land	Mixed	Ocean
R^2	Before QA filter	MAIAC	0.859	0.693	**0.750**	**0.845**	**0.832**	**0.754**	0.621
		DT	**0.903**	**0.798**	0.370	0.696	-------	0.520	**0.876**
		DB	0.813	0.636	0.550	0.799	0.428	0.600	0.434
	After QA filter	MAIAC	0.860	0.770	**0.687**	**0.848**	**0.834**	**0.758**	0.834
		DT	**0.915**	**0.812**	0.038	0.579	-------	0.553	**0.838**
		DB	0.843	0.804	0.480	0.852	0.710	0.724	0.152
R	Before QA filter	MAIAC	0.932	0.874	**0.875**	**0.933**	**0.929**	0.875	0.796
		DT	**0.964**	**0.896**	0.726	0.934	-------	**0.898**	**0.939**
		DB	0.927	0.850	0.744	0.928	0.689	0.832	0.777
	After QA filter	MAIAC	0.933	0.904	**0.868**	**0.934**	**0.938**	**0.882**	0.921
		DT	**0.966**	**0.901**	0.585	0.916	-------	0.875	**0.941**
		DB	0.933	0.903	0.719	0.934	0.900	0.871	0.696
RMSE	Before QA filter	MAIAC	0.221	0.144	**0.085**	**0.195**	**0.109**	**0.163**	0.170
		DT	**0.178**	**0.131**	0.172	0.275	-------	0.246	**0.097**
		DB	0.276	0.174	0.155	0.239	0.214	0.244	0.210
	After QA filter	MAIAC	0.219	0.127	**0.114**	**0.194**	**0.110**	**0.161**	0.108
		DT	**0.173**	**0.124**	0.164	0.288	-------	0.223	**0.106**
		DB	0.228	0.122	0.191	0.159	0.170	0.177	0.208
Bias	Before QA filter	MAIAC	**-0.004**	0.066	-0.018	**0.030**	-0.046	**0.002**	0.021
		DT	0.065	**0.020**	0.048	0.201	-------	0.167	**0.006**
		DB	0.092	0.038	**0.011**	0.061	**-0.007**	0.057	-0.088

	After QA filter	MAIAC	**-0.007**	0.053	**0.051**	0.027	**-0.057**	0.011	**0.031**
		DT	0.064	**-0.003**	0.075	0.224	-------	0.114	-0.057
		DB	0.062	-0.020	-0.048	**0.019**	-0.092	**0.007**	-0.128
Within_EE	Before QA filter	MAIAC	**75.56**	43.09	**83.68**	**72.79**	**67.44**	**65.31**	67.96
		DT	71.12	56.23	47.19	24.36	-------	38.23	**81.11**
		DB	57.37	**64.41**	63.21	63.60	36.54	47.19	53.36
	After QA filter	MAIAC	**76.22**	47.75	46.02	**74.66**	**71.43**	**66.80**	**78.22**
		DT	72.67	56.53	37.04	19.33	-------	50.00	75.20
		DB	60.37	**72.20**	**60.41**	69.24	37.50	59.34	51.90

Table 4. Comparison retrieval accuracy of MAIAC, DT and DB product at different land cover types before and after QA filter.

Ångström exponent (AE) is key parameter to describe aerosol particles size and in general, local aerosol sources play a dominant role in aerosol regimes. We follow Martins et al., 2017's work to discover aerosol particles size in different land cover (Martins et al., 2017), Figure 6 shows scatterplot for AE (440nm-675nm) parameter versus AOD in different land cover type. Our results are similar with Martins et al., 2017's results. The aerosol types in China are mainly fine-mode aerosol particles (AE>1). Some coarse-mode particles (AE<0.5) are mainly in some sparse vegetation region, e.g. grassland (vegetation coverage in the selected site is less than 20%), built-up and unoccupied land. As observed in Figure 3, high AOD values mainly occurs in cropland and built-up areas. The aerosol types for these high AOD values are mainly fine-mode aerosol particles according to the AE parameter. Figure 7 presents AOD bias distribution along with AE parameter. Higher AOD bias often occurs when AODs are higher than 0.8 with 1<AE<1.5. There is no AE dependence when AOD are very small, e.g. lower than 0.1, for three product. However, it seems MAIAC has a more positive bias than DB product in very small level.

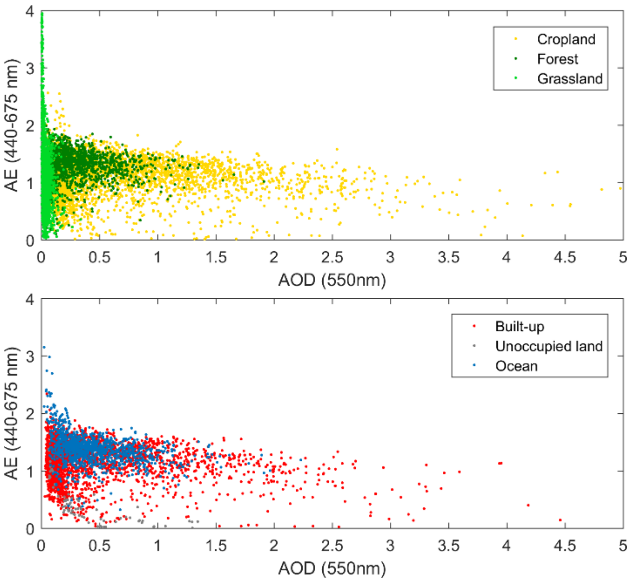

Figure 6. Scatterplot of AOD at 550nm against Ångström exponent with different land cover types. We select AERONET sites with maximum observations for each land cover type: Xianghe (cropland); Taipei_CWB (forest); QOMS_CAS (grassland); Beijing (built-up); Dunhuang (unoccupied land); Hong_Kong_PolyU (oceam).

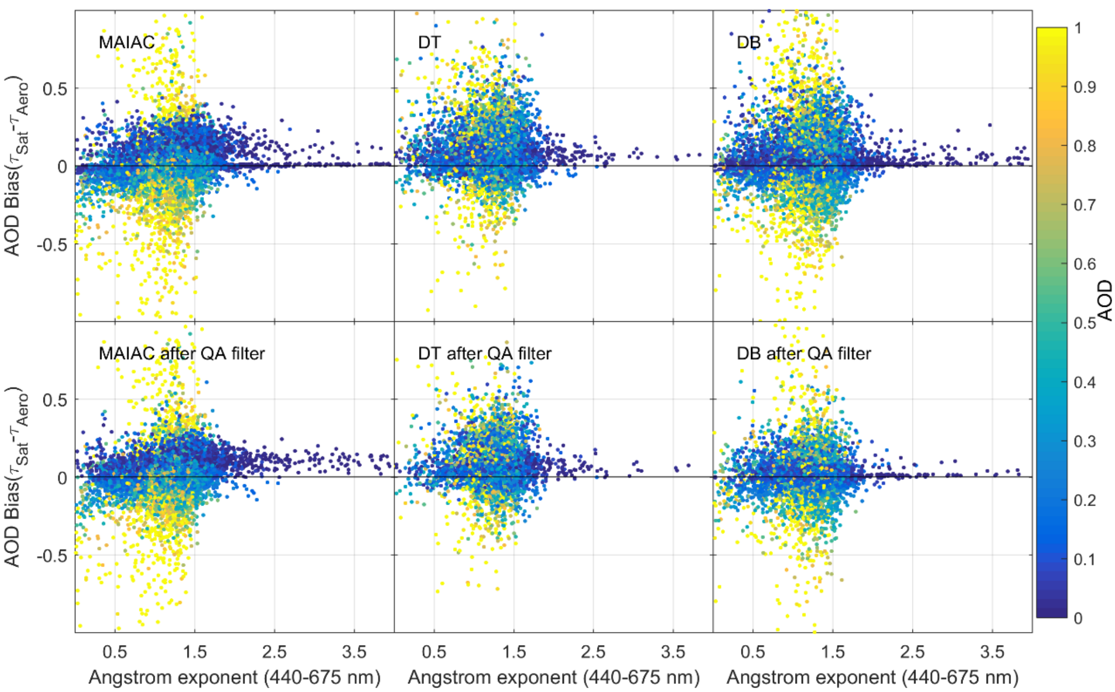

Figure 7. Scatterplot of AOD bias from matchup data versus AERONET Ångström exponent (440nm-675nm) before and after QA filter.

4.3 View geometry dependency analysis

In order to find out the how the view geometry influence the accuracy for three retrieval algorithms, we analyze view geometry dependency using the following four angles: solar zenith angle (SZA), view zenith angle (VZA), scattering angle (SA) and relative azimuth angle (RAA) (Superczynski et al., 2017). We separate each kind angle into 10 bins and statistic the AOD bias distribution in each bin. These results are displayed in Figure 8.

In terms of solar zenith angle, three retrieval algorithms all show strong dependency with different characteristic. A slight downtrend along with SZA is found in MAIAC algorithm, MAIAC retrievals seems slightly overestimated when SZA is less than 40° and underestimated when larger SZA is occurring. The mean biases only fluctuate from -0.05 and 0.05. For DT algorithm, the mean bias first rise when the SZAs are small and the mean bias reached the maximum at SZA≈25°. Then, the mean biases decreases as the SZA increases. The mean biases are close to zero when SZA arrives at the maximum value. With regard to DB algorithm, the mean bias first slowly decrease when SZAs are less than 35° and then rise rapidly as the SZA increases. After QA filter, the whole mean bias line moves down.

MAIAC and DB algorithm show no dependency with view zenith angle, the corresponding mean bias lines do not fluctuate much along with VZA. Compared with results before and after QA filter, the mean bias line for MAIAC algorithm slightly moves up and the mean bias line for DB algorithm moves down in a relatively great degree. VZA slightly affects DT performance with a little downtrend. After QA filter, the mean bias line slightly moves down.

Scattering Angle also greatly impacts the performance for three retrieval algorithms. MAIAC retrievals seem underestimated when SAs are less than 100° and slightly overestimated when SAs are between 100° and 155°. When SAs are larger than 155°, the retrievals tend to be underestimated. After QA filter, the corresponding retrievals at large SAs tend to be overestimated. For DT and DB retrievals, significant uptrend for mean bias along with SAs is found. Small positive biases are found when SAs are very small and large positive biases occur when SAs are very large. After QA filter, the significant uptrend is alleviated for DB retrievals. But large negative bias is found when SA approaches 180°. We consider the scarce matchup number of DB retrievals is the main reason for the negative bias.

For MAIAC algorithm, positive biases occur as the RAA approaches the extremes of 0°, 180° and negative bias emerge as RAA close to 90° where the matchup numbers are very limited in the three angle intervals. In the rest angle intervals, MAIAC shows no dependency with RAA. After QA filter, it seems a downtrend for mean bias along with RAA when backscattering (RAA<90°) occurs and an uptrend for mean bias when forward-scattering (RAA>90°) occurs. For DT algorithm, positive mean bias decreases as RAA increases at backscattering and first increases and then decreases at forward-scattering. After QA filter, the downward trend tends to alleviate at backscattering. For DB algorithm, at backscattering, the positive mean bias first decreases from very high to zero and then increases to slightly high. At forward-scattering, the positive mean biases are all larger than 0.05. After QA filter, at backscattering, there is no dependency with RAA for DB algorithm but most mean bias are lower than zero. At forward-scattering, an obvious linear downtrend from positive bias to negative bias as RAA increases.

Atmos. Chem. Phys. Discuss., https://doi.org/10.5194/acp-2018-1339
Manuscript under review for journal Atmos. Chem. Phys.
Discussion started: 25 January 2019

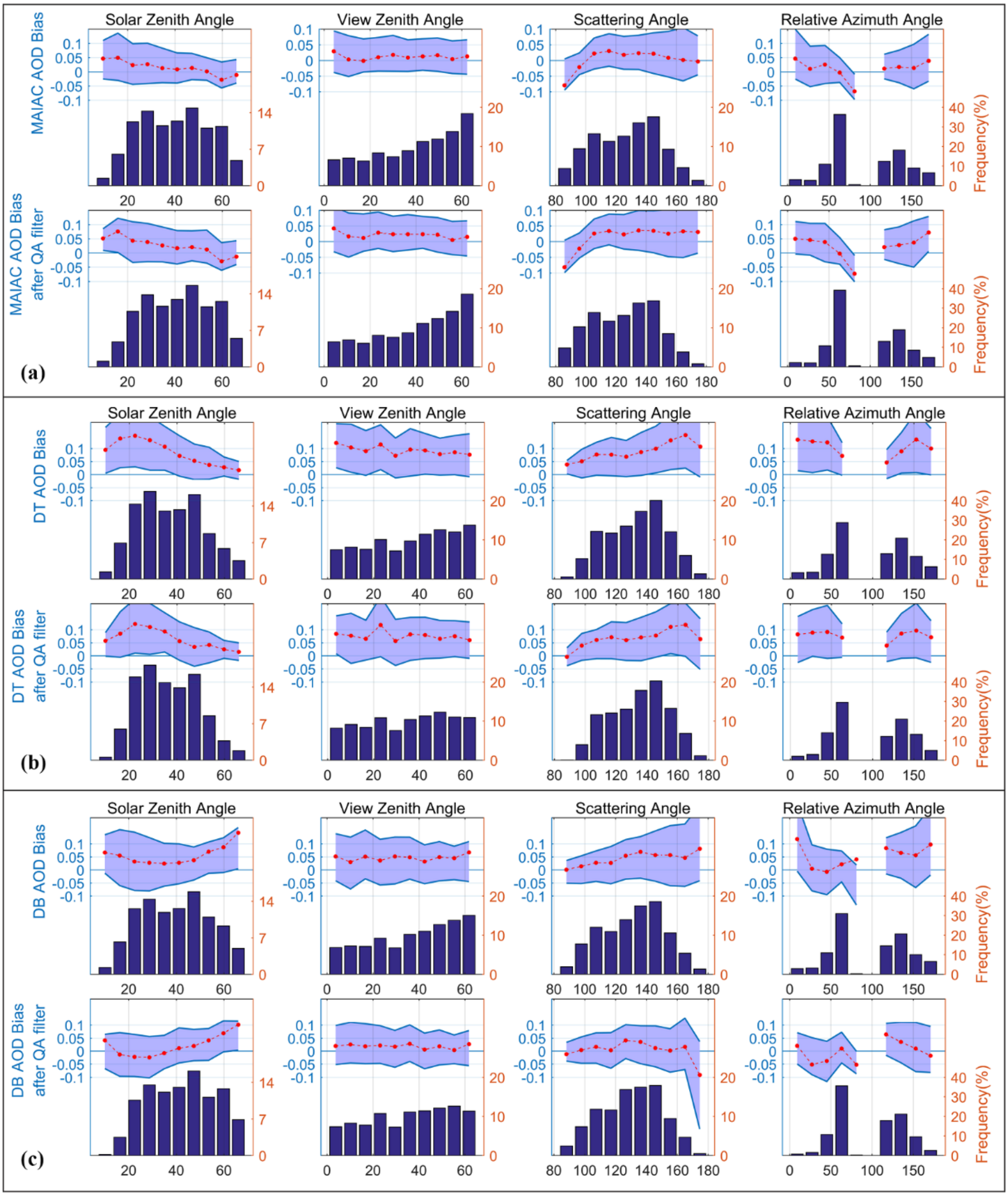

Figure 8. Dependency of AOD bias with solar zenith angle, view zenith angle, scattering angle and relative azimuth angle for (a) MAIAC product, (b) DT product and (c) DB product before and after QA filter. Dark blue bar is the histogram bin, red points in the shadow area are the mean bias of corresponding bin, the top and the bottom blue line are the 75% and 25% percentiles of AOD biases in the corresponding bin.

4.4 Analysis on spatiotemporal retrieval accuracy

To investigate three algorithms retrieval accuracy at different regions and different time, Figure 9 shows the R, RMSE, Bias and Within_EE results for each AERONET site and we ignore the sites with fewer than 10 matchup numbers due to few matchup numbers may cause unreliable statistical result.

Three products present different retrieval accuracies in different regions. In BTH region (marked by black box in Figure 1), three products show good correlation with ground measurements, e.g. R>0.9. But there are more retrievals for MAIAC and DT products falling within the EE limits than DB product. Based on Bias results, DT and DB products seem overestimated compared with MAIAC product. DT product is more positive biased compared with MAIAC product. In YRD region, the within_EE results show more MAIAC retrievals meet the EE limits than DT and DB product. Good correlation for three product also is found in this region. However, DT product is overestimated and DB is underestimated in this region. In the PRD region, MAIAC retrievals are obviously more accurate than DT and DB retrievals. The Within_EE results of MAIAC retrievals in this region are all higher than 70%. The Within_EE results of DT retrievals are relatively low for some sites before QA filter. After QA filter, the Within_EE results are greatly promoted. DB retrievals in this region won the worst performance with low Within_EE results, bad correlation and negative bias. In addition, MAIAC product are also the best accurate product in the NW area. The Within_EE and R results are overall higher than DT and DB products. And the RMSE results of MAIAC product in this region are also relatively low than ones of BTH and YRD region. The Within_EE results of MAIAC product for the most sites in the west of Taiwan are higher than 66% after QA filter, which shows high accuracy compared with DT and DB products. However, according to the east site, e.g. Lulin, the MAIAC retrievals seem overestimated with low Within_EE and R results. And DB retrievals in the Lulin site seem unbiased with high Within_EE (over 70%) and relatively high R (over 0.8) results. In the Tibet area, three algorithms all failed in retrieving AODs according to the statistical result due to high latitude and snow cover.

Figure 10 presents monthly validation results for three products. We ignore the specific QOMS_CAS site in this purpose due to its bad performance after QA filter and this will affect the overall accuracy. Three products show good correlation with ground measurements for all months with R>0.85. The AOD deviation for DT and MAIAC products is higher in spring and summer seasons than autumn and winter seasons which are consistent with the result of He et al., 2017 (He et al., 2017). The RMSE results for DB products are generally higher than DT and MAIAC products before QA filter. After QA filter, RMSE results are decreased with no obvious seasonal variability law. DT product seems a systematic overestimated and the positive biases are extremely high in spring and summer seasons. MAIAC product is positive biased during June to October with Bias<0.1. DB product is positive biased in all season before QA filter, however, the Bias results during June to October are significant reduced after QA filter. Before QA filter, the Within_EE results for MAIAC product are higher than ones of DT and DB products in all months. But there are less than 60% of MAIAC retrievals falling within the EE limits in summer season. After QA filter, the Within_EE results for DB product during June to September are superior to ones of MAIAC and DT products. The R^2 results for MAIAC products are stable for all months and most R^2 results are over 0.8. DB product has lower R^2 in the cold season during November to February and R^2 results in April and May for DT product are generally low than ones in other months. After QA filter, DB product achieve the higher R^2 results during April to September. According to matchup number results, MAIAC product has more matchup numbers than DT and DB product. However, all products have fewer matchup numbers in the summer season due to the increased cloud cover in the rainy season. In summary, MAIAC product are more accurate than DT and DB product expect for in summer season. In contrast with positive bias of MAIAC retrievals in summer season, the DB product after QA filter can achieve unbiased result with higher Within_EE and R^2 results than MAIAC product.

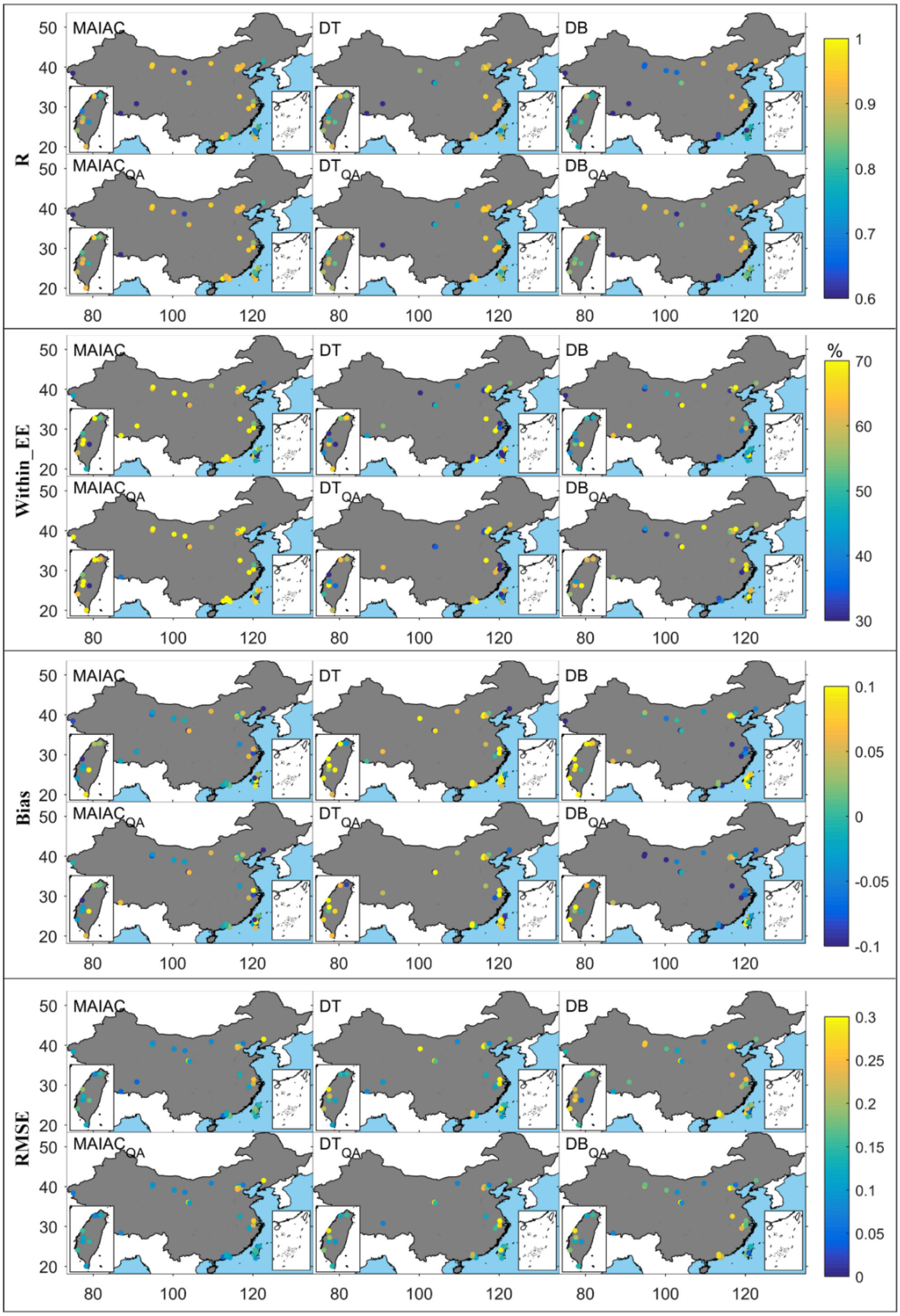

Figure 9. Evaluation result of MAIAC, DT, DB after and before QA filter in each AERONET site. The subscript QA means corresponding results after QA filter.

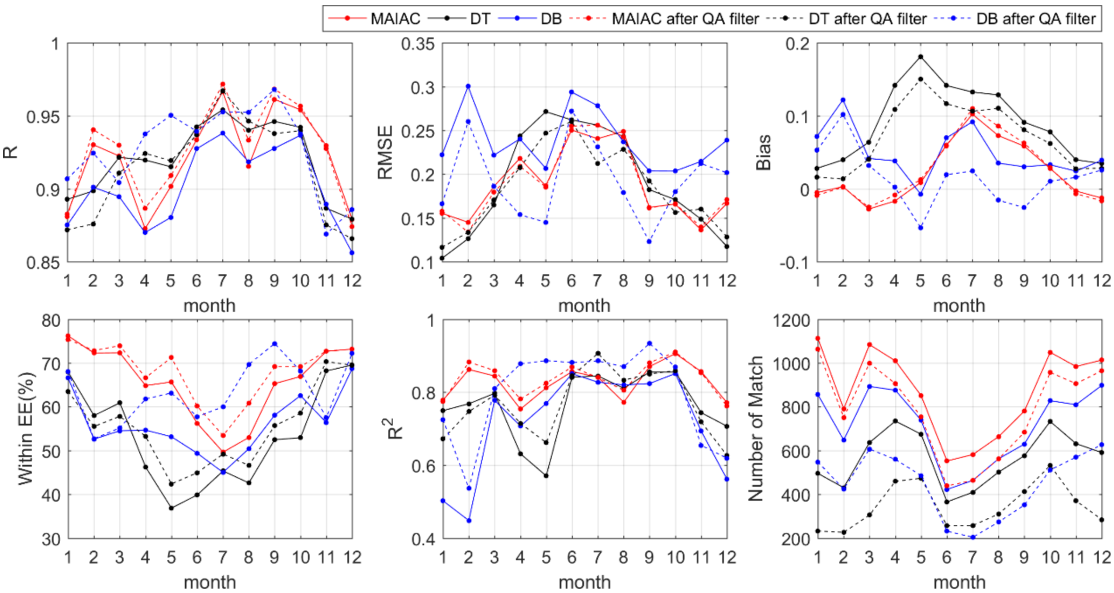

Figure 10. Validation of MAIAC, DT and DB in different months before and after QA filter

To investigate the annual change of retrieval accuracy for three products, Figure 11 shows corresponding statistical results for each year. Here, we ignore the results in the year of 2000, 2001, 2002 and 2003 due to less matchup number in these years. Three products show high correlation with ground measurements according to the R results. However, the accuracy for DB products have a sharp down in the 2009 with a slightly low R≈0.8. The MAIAC AOD deviation is generally small with which most RMSE results are lower than 0.2 and larger than 0.15. RMSE results of DB product are generally larger than 0.2 before QA filter. After QA filter, the RMSE results varies in a large range from 0.15 to 0.25. Based on the Bias result, there is a significant uptrend for three products as year increases. MAIAC Bias results are generally smaller than DT and DB product, and most Bias results for MAIAC product falls within ±0.05 with negative bias before 2010 and positive bias after 2010. From Within_EE results, MAIAC also shows better accuracy than DT and DB products and the Within_EE results have a slight declined trend as year increases. In terms of R2 results, MAIAC product is more stable and higher than DT and DB products. The matchup number for three products shows an increase trend due to more and more AERONET sites are stablished in China region as time goes on.

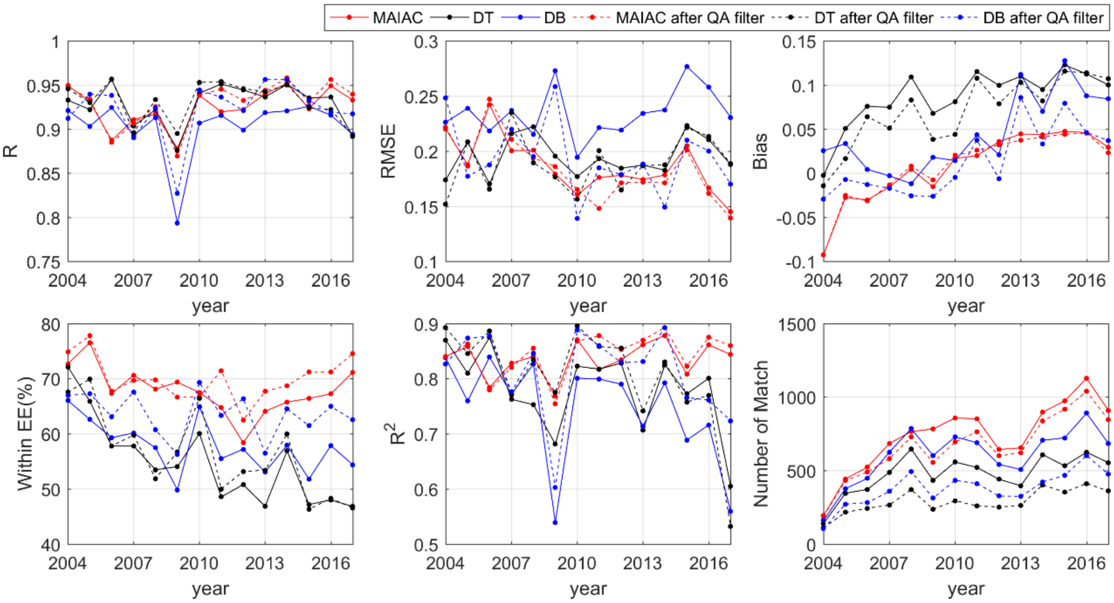

Figure 11. Validation of MAIAC, DT and DB in different years before and after QA filter

4.5 Analysis on spatial variation difference

To compare the difference in spatial variations for three products, we upscale MAIAC product to match the grid of DT and DB products, that is to say, 1 km pixels falling within the 10 km grid are averaged. Such protocol can help us to investigate the difference in different regions between three products.

Figure 12 presents multiyear averaged and difference results between MAIAC, DT and DB products, aerosol loading presents a noteworthy assembling characteristic. Higher AOD values concentrate at north China plain and Szechwan Basin where the land cover types are mainly cropland-oriented in Figure 1. Before QA filter, compared with DT and DB observations, MAIAC AODs are smaller in north China plain and larger in Yunnan province and the east of Taiwan. After QA filter, DB AODs become smaller in north China plain and southeast region. Compared with DB AODs, MAIAC AODs become slightly higher in north China plain (difference over 0.1) and obviously higher in southeast region of China (difference over 0.3). Recall the statistical result in Figure 9, DT and DB products are overestimated in BTH region, DB product are underestimated in the YRD region, and MAIAC product seems overestimated in the east of Taiwan. This indicates MAIAC retrievals are more accurate than DT and DB in the north China plain and southeast region, and DB retrievals are more accurate than MAIAC in the east of Taiwan. However, due to lack of AERONET site in Yunnan province, we cannot evaluate the accuracy for three products in the Yunnan province. Difference between before and after QA filter for MAIAC product is very small except for some individual pixels in Tibet region. In addition, there is an obvious boundary in the 30° Latitude according to AOD spatial variation difference subfigure between MAIAC and the other two products. This boundary is caused by the difference regional aerosol model used in the above and below the 30°Latitude (Lyapustin et al., 2018).

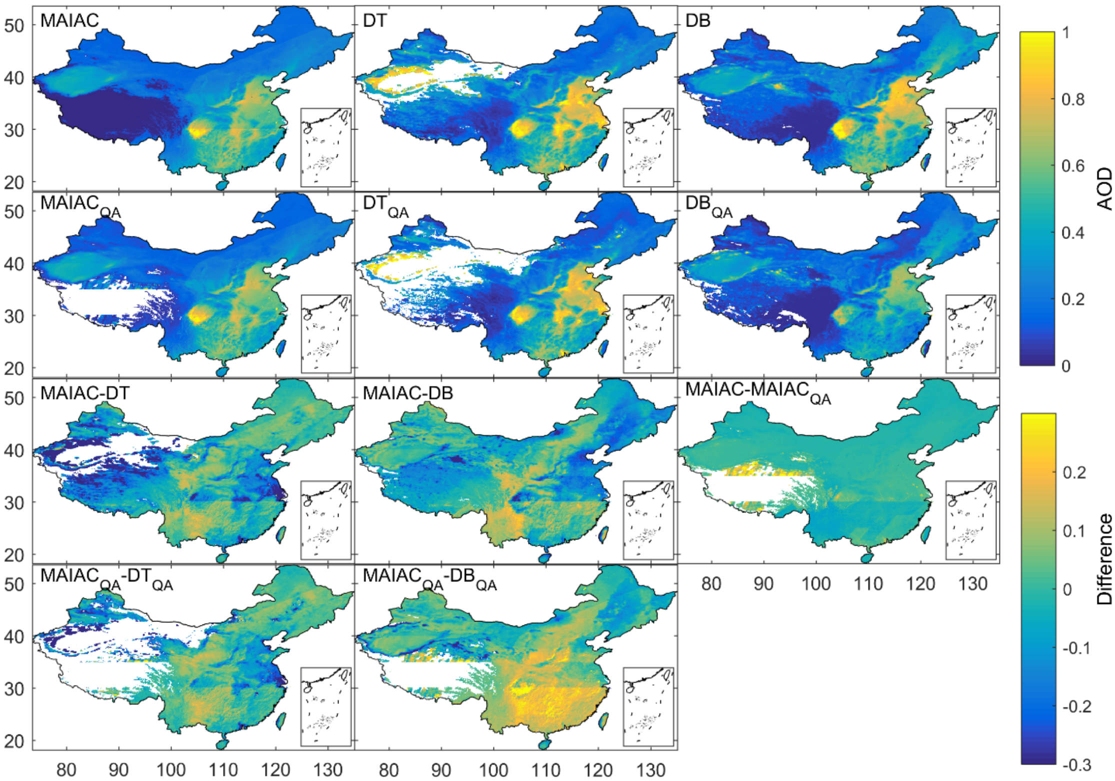

Figure 12. Averaged AOD distribution of all year for MAIAC, DT, DB before QA filter and their difference after QA filter. The subscript QA means corresponding results after QA filter.

Figure 13 and Figure 14 show the seasonal comparison results among three products before and after QA filter. The AOD spatial variation for three products show apparent seasonal characteristic. AODs in north China plain in summer season are higher than ones in other seasons and AODs in Tarim Basin in spring season are higher than ones in other seasons. Based on the AOD spatial variation difference map, the difference between MAIAC and DT in north China plain evolves gradually from negative in spring to positive in winter. The negative difference between MAIAC and DB in north China plain are higher in summer and winter than ones in spring and autumn. The positive difference in Yunnan province between MAIAC and DT is slightly lower than ones between MAIAC and DB. After QA filter, AODs in south of China for DB product are extremely low than ones for MAIAC product.

Atmos. Chem. Phys. Discuss., https://doi.org/10.5194/acp-2018-1339
Manuscript under review for journal Atmos. Chem. Phys.
Discussion started: 25 January 2019

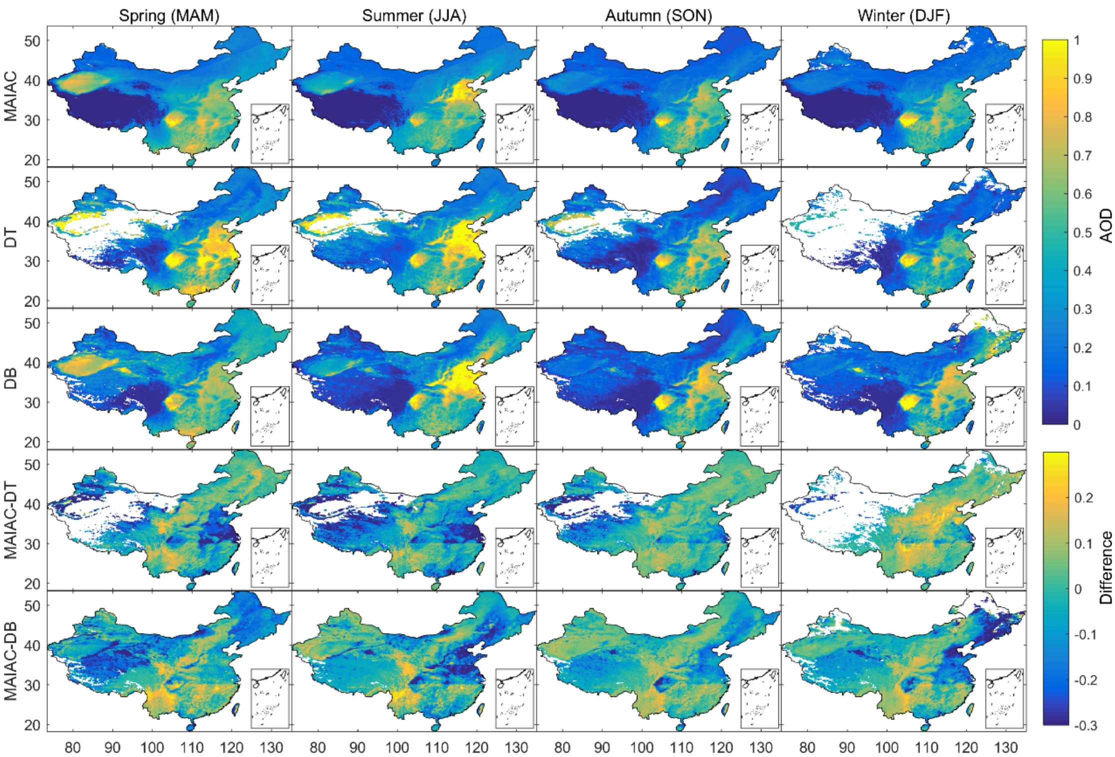

Figure 13. Seasonal averaged AOD distribution for MAIAC, DT, DB and their difference before QA filter. The subscript QA means corresponding results after QA filter.

Atmos. Chem. Phys. Discuss., https://doi.org/10.5194/acp-2018-1339
Manuscript under review for journal Atmos. Chem. Phys.
Discussion started: 25 January 2019

Atmospheric Chemistry and Physics
Open Access
Discussions
EGU

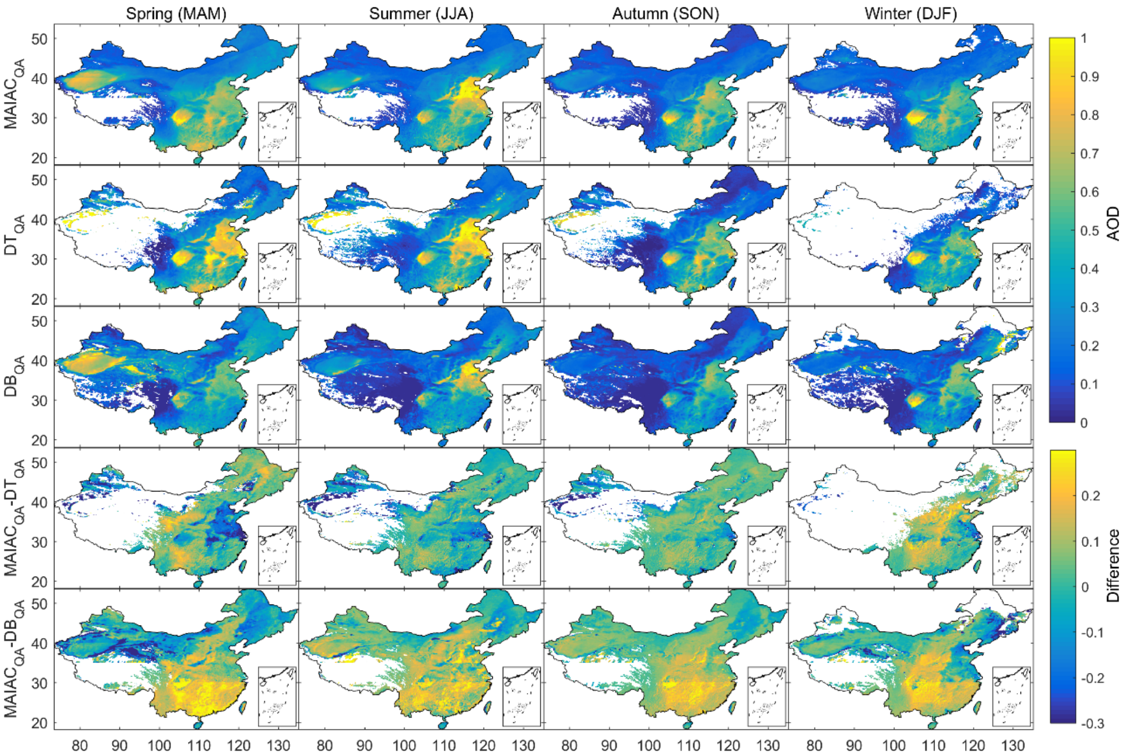

Figure 14. Seasonal averaged AOD distribution for MAIAC, DT, DB and their difference after QA filter. The subscript QA means corresponding results after QA filter.

4.6 Analysis on spatiotemporal completeness

Based the upscale MAIAC 10 km data in section 4.4, we calculate the daily spatial completeness by using the percentage of the available AOD pixel number over the total pixel number in China region and temporal completeness by using the percentage of the available AOD pixel number over the length of study period for each pixel in China region.

According to the Figure 15, the spatial completeness of MAIAC product is higher than ones of DT and DB products before and after QA filter. The spatial completeness of DT product is smallest due to its failure retrieval in bright surface. The spatial completeness for all product shows an obvious periodical trend change. Table 5 statistics the spatial completeness of three products in different seasons. Before QA filter, the averaged spatial completeness of MAIAC (46.87%) is higher than ones of DT (16.66%) and DB (34.80%). After QA filter, the declined proportion of MAIAC (17.18%) is more than ones of DB (15.30%) and DT (8.66%) due to many climatology values in Tibet Plateau are discarded. Compared spatial completeness in four seasons, the spatial completeness for three products in autumn is higher than other three seasons due to reduced cloudiness in the dry autumn season. The spatial completeness in winter is smallest by the influence of surface snow cover and large trees deciduous. Compared with MAIAC and DB products, the spatial completeness of DT product in winter season is minimal due to bright surface in winter.

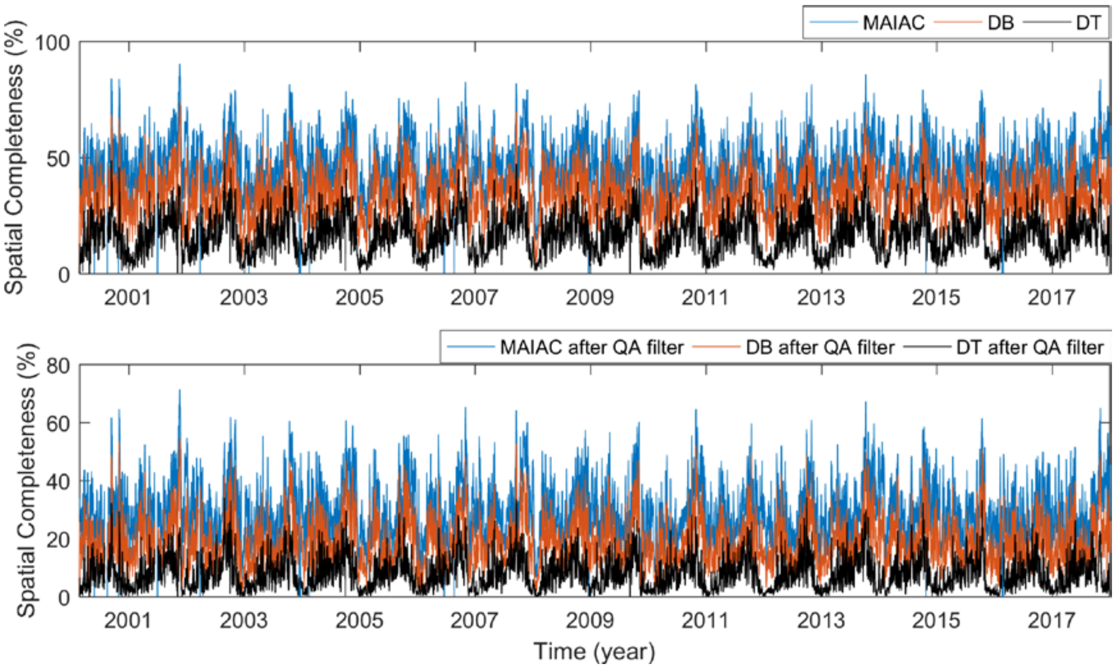

Figure 15. Daily spatial completeness for MAIAC, DT and DB from 2000 to 2017 before and after QA filter.

		All year	Spring	Summer	Autumn	Winter
Before QA filter	MAIAC	46.87	44.80	43.83	55.80	42.89
	DT	16.66	15.71	19.22	22.72	8.60
	DB	34.80	34.93	33.59	42.01	28.30
After QA filter	MAIAC	29.69	29.06	25.17	37.17	27.22
	DT	8.00	7.20	9.63	11.76	3.19
	DB	19.50	20.31	16.23	25.90	15.31
Declined Proportion	MAIAC	17.18	15.74	18.66	18.63	15.67
	DT	8.66	8.52	9.59	10.96	5.40
	DB	15.30	14.61	17.36	16.12	12.99

Table 5. Seasonal averaged spatial completeness for MAIAC, DT, DB before and after QA filter, and theirs declined proportion after QA filter

Figure 16 presents temporal completeness in China region for three products. Due to the filled climatology values in Tibet Plateau, the temporal completeness of MAIAC product in this region is very high (over 80%). After QA filter, the temporal completeness decreases rapidly in this region. In the other region, the declined proportions of temporal completeness for MAIAC are mostly lower than 10% except for Yunnan province (nearly 15%), Hainan province (nearly 20%) and the east of Taiwan (nearly 20%). Compared with MAIAC and DB product, DT retrievals in Tarim Basin are very scarce due to its failure in desert bright surface. DT retrievals more concentrate on north China plain and Yunan province. After QA filter, the severe dropped proportion area of temporal completeness (nearly 30%) for DT product is found in cropland region in the north east of China. The severe dropped proportion (nearly 40%) area for DB product after QA filter are mainly focus on unoccupied land, e.g. gobi, saline-alkali soil etc, in the top of Tibet Plateau. Compared with MAIAC product, before QA filter, DB product has more retrievals in Tarim Basin, north China plain and southeast region of China and less retrievals in Yunnan province and north east of China. After QA filter, the temporal completeness of MAIAC product is better than ones of DB product in all region.

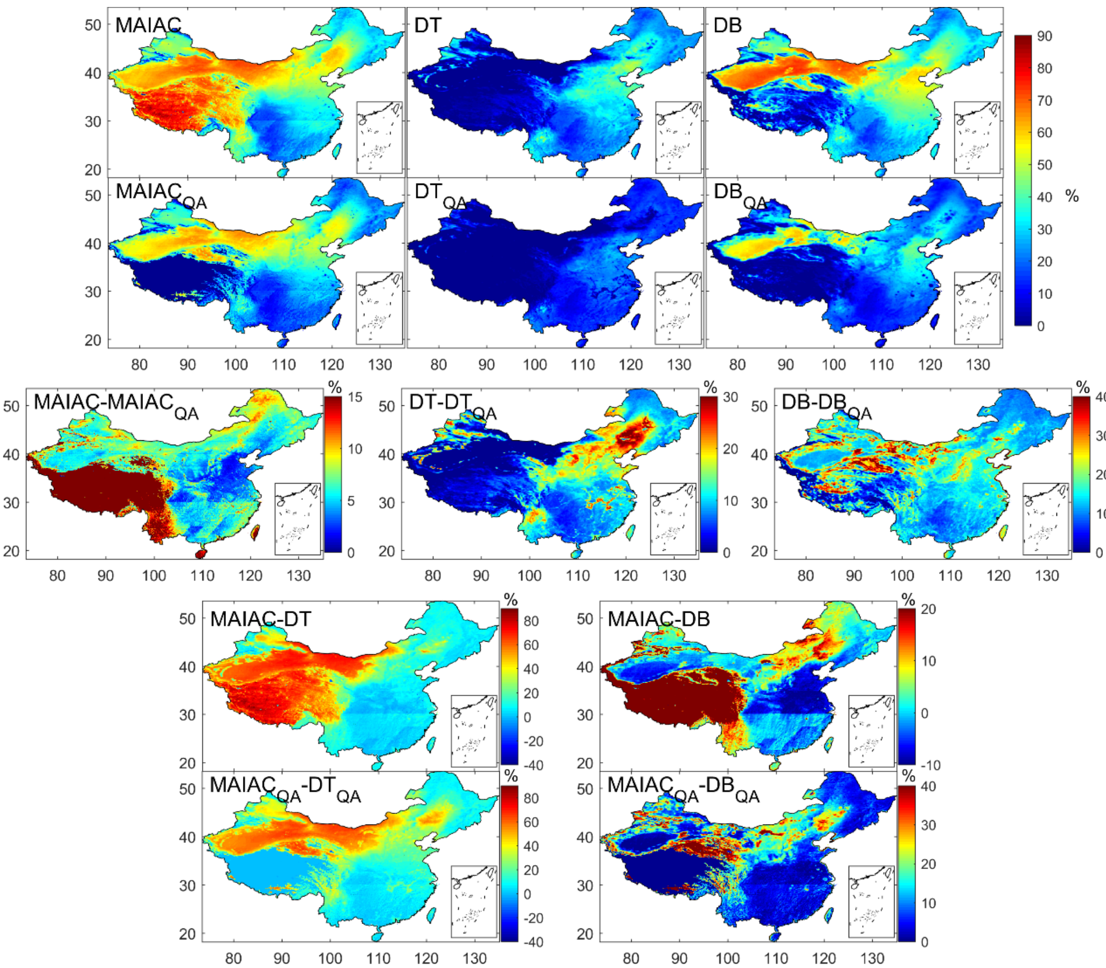

Figure 16. Spatial distribution of temporal completeness for MAIAC, DT, DB before and after QA filter and their difference. The subscript QA means corresponding results after QA filter.

5. Conclusion

In this study, we presents a first comprehensive validation and comparison for three MODIS aerosol retrieval algorithm (i.e. MAIAC, DT and DB) across the whole China from overall accuracy, land cover dependency, view geometry dependency, spatiotemporal retrieval accuracy, spatial distribution difference and spatiotemporal completeness aspects. These validation results may guide users to utilize three products appropriately. In terms of overall accuracy, MAIAC product is more accurate than DT and DB products. DT and DB products are positive biased before QA filter and the positive bias for DB product is alleviated by QA filter.

MAIAC retrievals show good correlation with ground measurements at different land cover types after QA filter. Compared with DT and DB products, DT retrievals in cropland, forest and ocean seem more accurate but with positive bias than retrievals by MAIAC and DB algorithms. MAIAC algorithm performs better in grassland, built-up and mixed areas than DT and DB algorithms.

Three algorithms show strong dependency with SZA, SA and RAA. VZA only affect little the retrieval accuracy of three algorithms. Mean bias decreases from positive to negative as SZA increase for MAIAC algorithm. For DT algorithm, the positive mean biases first increase and then decrease and DB algorithm present opposite trend compared with DT algorithm. SA mainly impacts MAIAC retrievals with negative bias when SAs are less than 100° and a significant uptrend is found as SA increases for DT and DB algorithm. After QA filter, the upward trend is alleviated for DB algorithm. Three algorithms show large uncertainties when RAA close to 90° and the extremes of 0° and 90° due to scare matchup number.

MAIAC product performs better in BTH, YRD, PRD and NW regions than DT and DB algorithm, the performance of DB product after QA filter in the east of Taiwan is better than DT and MAIAC products. According to validation in different month, MAIAC algorithm performs better than DT and DB algorithms in most months except for June, July, August and September. In these four months, MAIAC retrievals seem overestimated and DB retrievals after QA filter are more accurate than MAIAC retrievals. In the validation at year scale, MAIAC algorithm generally performs better than DT and DB algorithm. However, as year increases, an uptrend in mean bias was found for three algorithms.

Three AOD products present a similar spatial pattern with high aerosol loading in north China plain and Szechwan Basin. In comparison, MAIAC retrievals are lower in north China plain and Szechwan Basin than DT and DB retrievals, and higher in Yunnan province and the east of Taiwan province than DT and DB retrievals. After QA filter, DB AOD values are significantly reduced and obviously lower than MAIAC product in south east of China.

Based on the spatiotemporal completeness analysis, MAIAC product has more retrievals in spatiotemporal domain than DT and DB products. The spatial completeness exhibits strong periodical change, the temporal completeness is highest in autumn season than other season due to the declined cloud cover in this dry season and lowest in winter season due to snow cover and deciduous vegetation. In terms of temporal completeness, MAIAC has more retrievals in Tarim Basin and the cropland in the north east region of China compared with DT algorithm. Compared with DB algorithm, MAIAC has less retrievals in Tarim Basin and south east of China and more retrievals in north east of China. After QA filter, the temporal completeness of MAIAC in all region of China are better than DB product.

Author contribution

Ning Liu and Bin Zou designed the whole experiment. Ning Liu and Yu Liang developed the experiment code and performed it. The manuscript was initially written by Ning Liu and fully revised by Bin Zou. Huihui Feng and Yuqi Tang provided a lot of constructive comments on the experiment.

Acknowledgements

The authors thank the support of the National Key Research and Development Program of China (grant 2016YFC0206205) and the National Natural Science Foundation of China (grant 41871317).

References

Aerosol Dark Target (10km & 3km) Collection 6.1 Changes. available at: https://modis-atmosphere.gsfc.nasa.gov/sites/default/files/ModAtmo/C061_Aerosol_Dark_Target_v2.pdf, (last access: 14 December, 2018), 2017.

Changes to Modis Deep Blue Aerosol Products Betwwen Collection 6 and Collection 6.1, available at: https://modis-atmosphere.gsfc.nasa.gov/sites/default/files/ModAtmo/modis_deep_blue_c61_changes2.pdf, (last access: 14 December, 2018), 2017.

Chu, D. A., Kaufman, Y. J., Ichoku, C., Remer, L. A., Tanre, D., and Holben, B. N.: Validation of MODIS aerosol optical depth retrieval over land, Geophys. Res. Lett., 29, 1617, https://doi.rog/10.1029/2001GL013205, 2002.

Dominici, F., Greenstone, M., and Sunstein, C. R.: Particulate matter matters. Science, 344, 257-259, https://doi.rog/10.1126/science.1247348, 2014.

Eck, T. F., Holben, B. N., Reid, J. S., Dubovik, O., Smirnov, A., O'Neill, N. T., Slutsker, I., and Kinne, S.: Wavelength dependence of the optical depth of biomass burning, urban, and desert dust aerosols, J. Geophys. Res.-Atmos., 104, 31333-31349, https://doi.rog/10.1029/1999JD900923, 1999.

Fang, X., Zou, B., Liu, X., Sternberg, T., and Zhai, L.: Satellite-based ground PM2.5 estimation using timely structure adaptive modeling, Remote Sens. Environ., 186, 152-163, https://doi.rog/10.1016/j.rse.2016.08.027, 2016.

Feng, H., and Zou, B.: A greening world enhances the surface-air temperature difference, Sci. Total Environ., 658, 385-394, 2019

Gupta, P., Levy, R. C., Mattoo, S., Remer, L. A., and Munchak, L. A.: A surface reflectance scheme for retrieving aerosol optical depth over urban surfaces in MODIS dark target retrieval algorithm, Atmos. Meas. Tech., 9, 3293-3308, https://doi.rog/10.5194/amt-9-3293-2016, 2016.

He, Q., Zhang, M., Huang, B., and Tong, X.: MODIS 3 km and 10 km aerosol optical depth for China: Evaluation and comparison, Atmos. Environ., 153, 150-162, https://doi.rog/10.1016/j.atmosenv.2017.01.023, 2017.

He, Q., and Huang, B.: Satellite-based mapping of daily high-resolution ground PM2.5 in China via space-time regression modeling, Remote Sens. Environ., 206, 72-83, https://doi.rog/10.1016/j.rse.2017.12.018, 2018.

He, Q., Huang, B.: Satellite-based high-resolution PM2.5, estimation over the Beijing-Tianjin-Hebei region of China using an improved geographically and temporally weighted regression model, Environ. Pollut., 236, 1027-1037, https://doi.rog/10.1016/j.envpol.2018.01.053, 2018.

Hsu, N. C., Tsay, S. C., King, M..D., and Herman, J. R.: Aerosol properties over bright-reflecting source regions, IEEE Trans. Geosci. Remote Sensing, 42, 557-569, https://doi.rog/10.1109/TGRS.2004.824067, 2004.

Hsu, N. C., Jeong, M. J., Bettenhausen, C., Sayer, A. M., Hansell, R., Seftor, C. S., Huang, J., and Tsay, S. C.: Enhanced Deep Blue aerosol retrieval algorithm: The second generation, J. Geophys. Res.-Atmos., 118, 9296-9315, https://doi.rog/10.1002/jgrd.50712, 2013.

Ichoku, C., Chu, D. A., Mattoo, S., Kaufman, Y. J., Remer, L. A.. Tanré, D., Slutsker, I., and Holben, B. N.: A spatio-temporal approach for global validation and analysis of MODIS aerosol products, Geophys. Res. Lett., 29, 1616, https://doi.rog/10.1029/2001GL013206, 2002.

Kaufman, Y. J., Tanré, D., Remer, L. A., Vermote, E. F., Chu, A. and Holben, B. N.: Operational remote sensing of tropospheric aerosol over land from EOS moderate resolution imaging spectroradiometer, J. Geophys. Res.-Atmos., 102, 17051–17067, https://doi.rog/10.1029/96JD03988, 1997.

Levy, R. C., Remer, L. A., Kleidman, R. G., Mattoo, S., Ichoku, C., Kahn, R. and Eck T. F.: Global evaluation of the Collection 5 MODIS dark-target aerosol products over land, Atmos. Chem. Phys., 10, 10399–10420, https://doi.rog/10.5194/acp-10-10399-2010, 2010.

Levy, R. C., Mattoo, S., Munchak, L. A., Remer, L. A., and Sayer, A. M.: The Collection 6 MODIS aerosol products over land and ocean, Atmos. Meas. Tech., 6, 2989-3034, https://doi.rog/10.5194/amt-6-2989-2013, 2013.

Li, L., Zhang, J., Meng, X., Fang, Y., Ge, Y., Wang, J., Wang, C., Wu, J., and Kan, H.: Estimation of PM2.5 concentrations at a high spatiotemporal resolution using constrained mixed-effect bagging models with MAIAC aerosol optical depth, Remote Sens. Environ., 217, 573-586, https://doi.rog/10.1016/j.rse.2018.09.001, 2018.

Lucht, W., Schaaf, C. B., and Strahler A. H.: An algorithm for the retrieval of albedo from space using semiempirical BRDF models, IEEE Trans. Geosci. Remote Sens., 38, 977–998, https://doi.rog/10.1109/36.841980, 2000.

Lyapustin, A., Wang, Y., Laszlo, I., Kahn, R., Korkin, S., Remer, L., Levy, R., and Reid, J. S.: Multiangle implementation of atmospheric correction (MAIAC): 2. Aerosol algorithm, J. Geophys. Res.-Atmos., 116, D03211, https://doi.rog/10.1029/2010JD014986, 2011.

Lyapustin, A., Wangm Y., Korkin, S., and Huang, D.: MODIS Collection 6 MAIAC algorithm, Atmos. Meas. Tech., 11, 5741–5765, https://doi.rog/10.5194/amt-11-5741-2018, 2018.

Ma, Z., Hu, X., Huang, L., Bi J., and Liu Y.: Estimating Ground-Level PM2.5 in China Using Satellite Remote Sensing, Environ. Sci. Technol., 48, 7436-7444, https://doi.rog/10.1021/es5009399, 2014.

Martins, V. S., Lyapustin, A., de Carvalho, L. A. S., Barbosa, C. C. F., and Novo, E. M. L. M.: Validation of high-resolution MAIAC aerosol product over South America, J. Geophys. Res.-Atmos., 122, 7537-7559, https://doi.rog/10.1002/2016JD026301, 2017.

Qian, Y., and Giorgi, F.: Interactive coupling of regional climate and sulfate aerosol models over eastern Asia, J. Geophys. Res.-Atmos., 104, 6477-6499, https://doi.org/10.1029/98JD02347, 1999.

Rajeev, K., and Ramanathan, V.: Direct observations of clear-sky aerosol radiative forcing from space during the Indian Ocean Experiment, J. Geophys. Res.-Atmos., 106, 17221-17235, https://doi.org/10.1029/2000JD900723, 2001.

Remer, L. A., Kaufman, Y. J., Tanre, D., Mattoo, S., Chu, D. A., Martins, J. V., Li, R. R., Ichoku, C., Levy, R. C., Kleidman, R. G., Eck, T. F., Vermote, E., and Holben, B. N.: The MODIS aerosol algorithm, products, and validation, J. Atmos. Sci., 62, 947–973, https://doi.rog/10.1175/JAS3385.1, 2005.

Remer, L. A., Mattoo, S., Levy, R. C., and Munchak, L. A.: MODIS 3 km aerosol product: Algorithm and global perspective, Atmos. Meas. Tech., 6, 1829-1844, https://doi.rog/10.5194/amt-6-1829-2013, 2013.

Salomonson, V. V., Barnes, W. L., Maymon, P. W., Montgomery, H. E., and Ostrow, H.: MODIS: Advanced facility instrument for studies of the Earth as a system, IEEE Trans. Geosci. Remote Sensing, 27, 145-153, https://doi.rog/10.1109/36.20292, 1987.

Superczynski, S. D., Kondragunta, S., Kondragunta, S., and Lyapustin, A.: Evaluation of the Multi-Angle Implementation of Atmospheric Correction (MAIAC) Aerosol Algorithm through Intercomparison with VIIRS Aerosol Products and AERONET: MAIAC AOT Evaluation, J. Geophys. Res.-Atmos., 122, 3005-3022, https://doi.rog/10.1002/2016JD025720, 2017.

Xiao, Q., Wang, Y., Chang, H. H., Meng, X., Geng, G., Lyapustin, A., and Liu, Y.: Full-coverage high-resolution daily PM2.5 estimation using MAIAC AOD in the Yangtze River Delta of China, Remote Sens. Environ., 199, 437-446, https://doi.rog/10.1016/j.rse.2017.07.023, 2017.

Xu, S., Zou, B., Shafi, S., and Sternberg, T.: A hybrid Grey-Markov/ LUR model for PM10 concentration prediction under future urban scenarios, Atmos. Environ., 187, 401-409, https://doi.org/10.1016/j.atmosenv.2018.06.014, 2018.

Zhai, L., Li, S., Zou, B., Sang, H., Fang, X., and Xu, S.: An improved geographically weighted regression model for PM2.5 concentration estimation in large areas, Atmos. Environ., 181, 145–154, https://doi.org/10.1016/j.atmosenv.2018.03.017, 2018.

Zhang, G., Li, J., Li, X., Xu, Y., Guo, L., Tang, J., Lee, C. S. L., Liu, X., and Chen, Y.: Impact of anthropogenic emissions and open biomass burning on regional carbonaceous aerosols in South China, Environ. Pollut., 158, 3392-3400, https://doi.rog/10.1016/j.envpol.2010.07036, 2010.

Zou, B., Pu, Q., Bilal, M., Weng, Q., Zhai, L., and Nichol, J. E.: High-Resolution Satellite Mapping of Fine Particulates Based on Geographically Weighted Regression, IEEE Geosci. Remote Sens. Lett., 13, 495–499, https://doi.org/10.1109/LGRS.2016.2520480, 2016.

Zou, B., You, J., Lin, Y., Duan, X., Zhao, X., Xin, F., Campen M.J., and Li, S.: Air pollution intervention and life-saving effect in China, Environ. Int. (in press). https://doi.org/10.1016/j.envint.2018.10.045, 2019.